

# Dynamic Loading and Stress Analysis of Tank Track Pad using Finite Element Method



Author

Syed Rashid Hussain Chishti

0000359181

Supervisor

Dr. Imran Akhtar

DEPARTMENT OF MECHANICAL ENGINEERING  
COLLEGE OF ELECTRICAL & MECHANICAL ENGINEERING  
NATIONAL UNIVERSITY OF SCIENCES & TECHNOLOGY  
ISLAMABAD  
FEBRUARY, 2023

Dynamic Loading and Stress Analysis of Tank Track Pad using Finite  
Element Method

Author

Syed Rashid Hussain Chishti

0000359181

A thesis submitted in partial fulfillment of the requirements for the degree of  
MS Mechanical Engineering

Thesis Supervisor

Dr. Imran Akhtar

Thesis Supervisor's Signature: \_\_\_\_\_

DEPARTMENT OF MECHANICAL ENGINEERING  
COLLEGE OF ELECTRICAL & MECHANICAL ENGINEERING  
NATIONAL UNIVERSITY OF SCIENCES & TECHNOLOGY  
ISLAMABAD  
FEBRUARY, 2023

## **Declaration**

I certify that this research work titled *Dynamic Loading and Stress Analysis of Tank Track Pad using Finite Element Method* is my own work. The work has not been presented elsewhere for assessment. The material that has been used from other sources, has been properly acknowledged / referred.

Signature of Student

Syed Rashid Hussain Chishti

2020-NUST-MS-ME-0000359181

## **Language Correctness Certificate**

This thesis has been read by an English expert and is free of typing, syntax, semantic, grammatical and spelling mistakes. Thesis is also according to the format given by the university.

Signature of Student

Syed Rashid Hussain Chishti

Registration Number

00000359181

Signature of Supervisor

Dr. Imran Akhtar

## **Plagiarism Certificate (Turnitin Report)**

This thesis has been checked for Plagiarism. Turnitin report endorsed by Supervisor is attached.

Signature of Student

Syed Rashid Hussain Chishti

Registration Number

00000359181

Signature of Supervisor

Dr. Imran Akhtar

## **Copyright Statement**

- Copyright in text of this thesis rests with the student author. Copies (by any process) either in full, or of extracts, may be made only in accordance with instructions given by the author and lodged in the Library of NUST College of E&ME. Details may be obtained by the Librarian. This page must form part of any such copies made. Further copies (by any process) may not be made without the permission (in writing) of the author.
- The ownership of any intellectual property rights which may be described in this thesis is vested in NUST College of E&ME, subject to any prior agreement to the contrary, and may not be made available for use by third parties without the written permission of the College of E&ME, which will prescribe the terms and conditions of any such agreement.
- Further information on the conditions under which disclosures and exploitation may take place is available from the Library of NUST College of E&ME, Rawalpindi.

## Certificate of Completeness

It is hereby certified that the dissertation submitted by NS Syed Rashid Hussain Chishti, Regn No. **00000359181** Titled: **Dynamic loading and stress analysis of tank track pad using finite element method**, has been checked/reviewed and its contents are complete in all respects.

Supervisor's Name: Dr. Imran Akhtar

Signature: \_\_\_\_\_

Date: \_\_\_\_\_

## **Acknowledgments**

First and foremost, I am thankful to my Creator Allah The Most High, to have guided me throughout this work at every step and for every new thought which You setup in my mind to improve it. Indeed, I could have done nothing without Your priceless help and guidance. Whosoever helped me throughout the course of my thesis, whether my parents or any other individual was Your will, so indeed none be worthy of praise but You.

I am profusely thankful to my beloved parents who raised me when I was not capable to make a walk and continued to support me throughout in every walk of my life, and for their continuous prayers for me.

I would also like to express special thanks to my Supervisor Dr. Imran Akhtar for being an inspiration and guidance throughout. He was always approachable and gave great advice during the ups and downs of my work. This thesis would not have been completed without his excellent and encouraging support.

I would also like to thank members of guidance and evaluation committee, Dr. Aamer Ahmed Baqai and Dr. Zafar Abbas Bangash for being always available to answer questions related to my research work and providing me necessary guidance at the right time. Even though they had no responsibility towards me, they always responded promptly. I am thankful to Dr. Imran Akhter for providing me the support of High-Performance Computing Center (HP2C) at College of E&ME for completing my simulations of the research work.

I extend my special thanks to Mr. Fahad Rafi Butt, Research Assistant at the Department of Mechanical Engineering, for sparing time to help me in skill development and for being there for me as a guide. I also owe my gratitude to my colleagues who enabled me to tread through the learning curve and develop reasonable expertise within a very short time frame. I am also thankful to myself for not giving up during all the hardships I faced during the course of this research.

Finally, I extend my deepest gratitude to Allah for providing me the opportunity and the ability to undertake this research.



# Dynamic Loading and Stress Analysis of Tank Track Pad using Finite Element Method

Syed Rashid Hussain Chishti

Dissertation submitted to the Faculty of the Department of Mechanical Engineering,

College of Electrical & Mechanical Engineering,

National University of Sciences & Technology (NUST)

in partial fulfillment of the requirements for the degree of

Master of Science

in

Mechanical Engineering

Dr. Imran Akhtar, Supervisor

Dr. Aamer Ahmed Baqai

Dr. Zafar Abbas Bangash

February, 2023

College of Electrical & Mechanical Engineering,

National University of Sciences & Technology (NUST), Islamabad

# Dynamic Loading and Stress Analysis of Tank Track Pad using Finite Element Method

Syed Rashid Hussain Chishti

## Abstract

Structural analysis is important for analyzing any structure for stability under all types of loadings. It determines the deformational behavior of structure and helps in realizing the life of structure. Finite element analysis is a numerical method used in this work for structural analysis of an armored tank track pad. Pak Army is in the continuous indigenization process, endeavors to reduce reliance on imports. A heavy fleet of armored main battle tanks are part of Pak Army. Modern armored tanks and other tracked vehicles use track pads to reduce vibrations, noise, road damage and to provide better traction. These track pads undergo frequent failures due to abrasion, chunking, deep cuts and scooping etc. The premature failure of these pads increases the import bill. The material and shape play a significant role towards life of the track pad. In this research work, finding a better track pad design for armored tracked vehicles is targeted. The work involves stress analysis through finite element method. Static structural analysis is performed with compressive loadings and dynamic analysis for constant speed operation is performed with compressive and shearing forces. Focus is laid on stress reduction by changing materials and varying shape. Four types of materials and seven different shapes are compared through finite element analysis. A better design of track pad is suggested as outcome at the end of the work which proves that the original design is not an optimized design.

**Keywords:** Finite Element Analysis, Dynamic Loading, Stress Analysis, Track Pad, Elastomers.

*Dedicated to the brave sons and daughters of the nation.*

## Table of Contents

<b>Declaration</b> .....	<b>iii</b>
<b>Language Correctness Certificate</b> .....	<b>iv</b>
<b>Plagiarism Certificate (Turnitin Report)</b> .....	<b>v</b>
<b>Copyright Statement</b> .....	<b>vi</b>
<b>Certificate of Completeness</b> .....	<b>vii</b>
<b>Acknowledgments</b> .....	<b>viii</b>
<b>Abstract</b> .....	<b>x</b>
<b>List of Figures</b> .....	<b>xv</b>
<b>List of Tables</b> .....	<b>xvii</b>
<b>List of Abbreviations</b> .....	<b>xviii</b>
<b>1 Introduction and Motivation</b> .....	<b>1</b>
1.1 Problem Statement .....	2
1.2 Motivation .....	2
1.3 Objectives of the Study .....	3
1.4 Organization of the Thesis .....	4
<b>2 Literature Review</b> .....	<b>5</b>
2.1 Literature Survey.....	5
2.1.1 Development and Fabrication of Track Pads.....	5
2.1.2 Dynamic Loads Impact on Tank Track .....	5
2.1.3 Thermographic Scanning of Track Pads.....	6
2.1.4 Exploring the Meta-materials .....	7
2.1.5 Terramechanics Models .....	13
2.1.6 Tracked Vehicle Model (FEM).....	14
2.1.7 Dynamic Forces of Weapon System (FEM).....	16
2.1.8 Rubber Pad Buffer of a Track Type Bulldozer .....	17
2.2 Research Gap.....	17
<b>3 Methodology</b> .....	<b>18</b>
3.1 Model Development.....	18

3.1.1	Dynamic Loading Model .....	18
3.1.2	Static Loading Model.....	18
3.2	Material Selection and Validation of Rubber Material .....	20
3.2.1	Experimental Test .....	20
3.2.2	Modeling in ANSYS.....	20
3.3	Mesh Independence.....	24
<b>4</b>	<b>FEA Results .....</b>	<b>26</b>
4.1	Materials Comparison at Static Loads and Varying Loads.....	26
4.1.1	Material Comparison as per ASTM D-412.....	26
4.1.2	Material Comparison on Static Loading Model.....	28
4.2	Shape Comparison.....	30
4.2.1	Original Pad Design.....	30
4.2.2	3-Cuts Pad Design.....	32
4.2.3	4-Cuts Pad Design.....	33
4.2.4	4-Lateral Cuts Pad Design .....	34
4.2.5	12-Cuts Pad Design.....	36
4.2.6	3-Extruded Slots Pad Design .....	37
4.2.7	Chevron Pad Design .....	38
<b>5</b>	<b>Analysis &amp; Discussion.....</b>	<b>41</b>
5.1	Material Analysis .....	41
5.1.1	Material Analysis of ASTM Coupon.....	41
5.1.2	Material Analysis of Static Loading Model.....	41
5.1.3	Recommended Material for Pad .....	42
5.2	Analysis of Shape Variants .....	42
5.2.1	Shape Analysis of Static Loading Models .....	42
5.2.2	Stress in Steel Track Body .....	43
5.2.3	Chevron Pad vs Original Pad Comparison .....	44

5.2.4	Recommended Shape.....	48
5.3	Dynamic Loading Analysis.....	48
<b>6</b>	<b>Conclusion &amp; Future Work .....</b>	<b>51</b>
6.1	Conclusion.....	51
6.2	Future Work .....	52
	<b>References.....</b>	<b>53</b>

## List of Figures

Figure 3-1: Track Assembly Model.....	19
Figure 3-2: Static Analysis Model.....	19
Figure 3-3: Force & Fixed Support.....	19
Figure 3-4: Stress-Strain Curve of Rubber Material.....	21
Figure 3-5: Force-Deformation Curve.....	21
Figure 3-6: Rubber Coupon.....	22
Figure 3-7: Tensile Testing.....	22
Figure 3-8: Coupon Dimensions (mm).....	23
Figure 3-9: Tensile Coupon Model in ANSYS.....	23
Figure 3-10: Deformation Results.....	23
Figure 3-11: Mesh Independence.....	25
Figure 4-1: Material Comparison at Varying Loads (Load vs Deformation) –ASTM D-412	27
Figure 4-2: Material Comparison at Varying Loads (Load vs FoS) ASTM D-412.....	28
Figure 4-3: Material Comparison at Varying Loads (Stress vs Strain) ASTM D-412.....	28
Figure 4-4: Material Comparison at Varying Loads (Load vs Deformation).....	29
Figure 4-5: Material Comparison at Varying Loads (Load vs FoS).....	29
Figure 4-6: Original Pad Ground Side.....	31
Figure 4-7: Original Pad Ground Side Results.....	31
Figure 4-8: Original Pad Results.....	31
Figure 4-9: 3-Cuts Pad.....	32
Figure 4-10: 3-Cuts Pad Ground Side Stress Contours.....	32
Figure 4-11: 3-Cuts Pad Stress Contours.....	33
Figure 4-12: 4-Cuts Pad.....	33
Figure 4-13: 4-Cuts Pad Ground Side Stress Contours.....	34
Figure 4-14: 4-Cuts Pad Stress Contours.....	34

Figure 4-15: 4-Lateral Cuts Pad.....	35
Figure 4-16: 4-Lateral Cuts Pad Ground Side Stress Contours .....	35
Figure 4-17: 4-Lateral Cuts Pad Stress Contours .....	35
Figure 4-18: 12-Cuts Pad .....	36
Figure 4-19: 12-Cuts Pad Ground Side Stress Contours .....	36
Figure 4-20: 12-Cuts Pad Stress Contours.....	37
Figure 4-21: 3-Extruded Slots Pad.....	37
Figure 4-22: 3-Extruded Slots Pad Ground Side Stress Contours .....	38
Figure 4-23: 3-Extruded Slots Pad Stress Contours .....	38
Figure 4-24: Chevron Pad.....	39
Figure 4-25: Chevron Pad Ground Side Stress Contours .....	39
Figure 4-26: Chevron Pad Stress Contours.....	40
Figure 5-1: Original Pad Design Steel Body .....	44
Figure 5-2: Chevron Pad Design Steel Body.....	44
Figure 5-3: Original Pad Groundside Stress Contours .....	45
Figure 5-4: Chevron Pad Groundside Stress Contours .....	46
Figure 5-5: Chevron Pad Groundside Stress Iso Lines.....	46
Figure 5-6: Original Design Steel Body Stress Contours .....	47
Figure 5-7: Chevron Design Steel Body Stress Contours.....	48
Figure 5-8: Dynamic Loading Model with Applied Forces.....	49
Figure 5-9: Maximum Stress in Dynamic Model .....	50
Figure 5-10: Maximum Stress in Central Track Pad .....	50



## **List of Tables**

Table 3-1: Tested Material Properties of Proprietary Rubber .....	20
Table 3-2: 1 <sup>st</sup> order Ogden Model Coefficients .....	24
Table 3-3: Deformation Variation in Experimental vs Simulation Results .....	24
Table 3-4: Mesh Independence Error .....	25
Table 4-1: Material Properties of Shortlisted Materials .....	27
Table 5-1: Shape Comparison.....	43

## List of Abbreviations

Air Defense Weapon System	-	ADWS
Styrene Butadiene Rubber	-	SBR
Unit Cell	-	UC
Unit Cell Synthesis	-	UCS
Modified Unit Cell Synthesis	-	MUCS
Representative Volume Element	-	RVE
Cantilever Beam	-	CB
Fixed Fixed Beam	-	FFB
Elemental Functional Geometries	-	EFG
Elemental Support Geometries	-	ESG
Armored Personal Carrier	-	APC
Finite Element Method	-	FEM
Finite Element Analysis	-	FEA
Factor of Safety	-	FoS

# Chapter 1

## Introduction and Motivation

Structural engineering is one of the earliest engineering since the time human civilization started to build their own houses, bridges and other structures. Structural analysis is significant in analyzing the structural stability. It ascertains whether the deformations faced by structure under loads is within permissible limit or otherwise and therefore ensures the failure of the design will not occur. Structural analysis determines the structural behavior under all types of loads. Structural analysis involves stability, vibration and strength analysis.

Structural analysis of rubber components is traditionally considered one of the most difficult area of solid mechanics. The foremost of challenges are due to a reliable definition of the so-called input parameters including material properties, load parameters, environmental and aging conditions, failure criteria, etc. Even if the designers are satisfied with the input information and are ready, they can expect a number of additional challenges when developing structural models. These additional challenges are primarily associated with quantitative analysis of such models. Computational efficiency of the required solution is another challenge. Rubber and elastomers are highly deformable thus large deformation is another aspect that adds to complications. Among other things, two fundamental problems in nonlinear structural analysis of rubber components are: to obtain computational convergence and to ensure that the solution is correct.

Structural analysis of rubber components is often complicated by significant geometrical non-linearity of deformation, incompressibility, complex constitutive models, and the contact nature of boundary/loading conditions. The last challenge is especially important due to high friction of rubber [1].

Finite element analysis is a popular method in recent times to perform structural analysis. It allows easier modeling of irregular shapes and complex geometries. It allows the designer to obtain the complicated solutions with relative ease in comparison to analytical solutions. This is one of the easiest numerical method. Designer has liberty to model the boundary conditions and obtain results with high accuracy. Results obtained from FEA are highly comprehensive and designers can easily point out trends and weaker areas of the model.

This research work involves application of finite element analysis on a track pad assembly. High speed armored track vehicles form important battle winning element of any army all over

the world. These track vehicles operate in all types of terrain and tracks of these vehicles sustain all types of loadings which includes tank weight and other dynamic loads. These tracks are fitted with track pads to reduce vibrations, noise, and track and road damage. The failures in these track pads is a frequent phenomenon and design improvements are being undertaken constantly.

The work is focused on finding a suitable track pad design for armored tracked vehicles. Static structural and transient structural analysis is performed with compressive loadings. Focus remains on stress reduction by changing materials and varying shape. Achievement of a suitable design of track pad is solicited as outcome.

## **1.1 Problem Statement**

Defense industries in Pakistan is endeavoring to develop tracks of armored vehicles. The quality of already developed track pads is not up to the mark and failure rate is quite high. Armored tanks undergo certain types of static and dynamic loadings during periods of rest, various tactical motions and gun firing, all these contributes towards deterioration of tank track pads and these track pads are required to be frequently replaced. Track pad failure leads towards damage of steel track assembly which significantly increases the cost of repair [2]. This opens up a research area for exploring the possibilities for use of better track pads having more life. In this research, focus is track pad analysis with all types of above stated loadings for groundside track pad to achieve a suitable track pad design. These loadings are required to be modelled and analyzed using finite element analysis. Track link assembly is modeled using ANSYS and static compressive loading derived from tank's weight is simulated. Dynamic load is estimated and will be simulated on a three pair pad-track link assembly.

## **1.2 Motivation**

Many of the army track vehicles uses elastomer track pads as it reduces vibrations, noise, road damage and provides better traction under certain road condition. A genuine tank track pad is used in this work for analysis, this pad is a full area track pad configuration with dual track pads assemblies joined through a track pin. When tank is in motion multiple dynamic loads acts on it due to asymmetric loading, gun firing and off road drive or driving on uneven surfaces. Moreover, static loading effects are also present during long periods of rest and refit. All these factors put strain on all tank track components and therefore requires analysis for its elastic limits and wear and tear during static and dynamic loads.

Most of the work in this area remains classified and therefore very little published literature is available with regards to development of tank track and related analysis. Harry and James [2] work for development and fabrication of elastomer track pads can be considered as baseline work. They successfully developed polyurethane formulations with improved display of properties. Pergantis [3] used the experimental technique to analyze various materials and two types of track pads using thermography, his work analyzed the track pads wear and tear through thermal scanning. Fatigue loading and hysteretic losses are major causes of heat buildup in track pads eventually causing the wear and tear of these pads. Wang et al. [4] analyzed hysteretic heat build up in a rubber pad buffer of a track type bulldozer and performed numerical simulations for three types of cases (a) earthmoving, (b) cutting and bulldozing and (c) loosening. Attempts are made by Satterfield and Kulkarni to develop a meta-material. UCS and MUCS are used to tessellate and form RVE (Representative volume element). The UCS and MUCS are then used to form a backer side trackpad for targeted deformation response and being further used for replacement in M1 Abram tank track. A dynamic analysis is performed by simulating a wheel roll over event over the track pad to analyze the backer pad [5]–[8].

Wear and tear in track pads have significant cost in repair of track systems and very less published literature is available for finite element analysis of track pads and no literature is available for analyzing groundside elastomer pad with FEM technique.

In this research, the track will be analyzed in comparison to genuine fitted sample, numerical analysis will be carried out for various stresses. The focus will remain on replacement of elastomer track pad. The research will not include experimental work on track assembly. The analysis will involve FEM techniques using ANSYS, where stress analysis will be performed with static and dynamic loading.

### **1.3 Objectives of the Study**

The general objective of this research work is to analyze and evaluate the track pad wear in order to generate a better design.

- a. To simulate static and dynamic loading on tank track pad assembly.
- b. To analyze wear in groundside tank track pad and steel track body.
- c. To suggest a better design for track pad.

Pakistan Army relies on imports for maintenance of hi tech equipment and a large chunk of national exchequer is expended in form of import bill. Promotion and capacity enhancement of

local industry is need of the hour and also a requirement by highest level. Reducing reliance on imports of these track pads is the need of the hour, a large sum is expended on procurement of these pads. Therefore, research in this area is the national need.

#### **1.4 Organization of the Thesis**

This thesis is organized into six different parts which include: introduction, literature review, methodology, FEA results, analysis and discussion, conclusion and future work. In the introduction part, the objectives, problem statement, motivation and significance are discussed. In part two, literature related to the topic is organized, research gap and research questions are discussed. In the third part, model development is discussed followed by validation of material that includes experimental testing, and finally this part includes mesh independence study of the model. In the fourth part, FEA is displayed for already discussed models with the view to find best material and shape. In the fifth part, analysis is made for obtaining the best material and shape, this part also includes dynamic loading analysis. Conclusion and future work is discussed in the final part.

## Chapter 2

### Literature Review

#### 2.1 Literature Survey

##### 2.1.1 Development and Fabrication of Track Pads

Harry and James [2] work with regards to development of elastomer can be considered as a baseline work. They concluded that track pads with better wear resistance can be developed, they further concluded that SBR track pads do not have considerable improvements for wear resistance, however the best choice they concluded is to use polyurethane elastomer formulations, all this was done as part of a study under TACOM. They successfully develop polyurethane elastomer formulations with better hysteretic properties, they overall improved material properties such as tear strength, hysteresis and abrasion. One of the formulation is developed into full tack pad and tested under TACOM for 100,000 cycles but no visual decomposition is observed after slicing. Molding procedures have significant impact on material properties of both polyurethane and SBR pads. They also suggested use of fibers in materials for enhancing material properties.

##### 2.1.2 Dynamic Loads Impact on Tank Track

Keays [9] conducted a case study for replacement of steel tracks of M113 vehicle with one made from aluminum alloy / SiC metal matrix composite, to achieve overall weight reduction of the vehicle. His work involved calculation of loads acting on the track which includes five types of loads namely initial tension, simple traction, frictional, inertial and vibrational loads. Exact initial tension cannot be measured accurately but for the analysis initial tension is estimated as 12 KN. Maximum drawbar pull of M113 vehicle is 110 KN. Traction on one side is therefore 55 KN. A 5 % margin for frictional loads is added which makes it 58 KN.

The weight of the vehicle is distributed through track wheels over the track. It is also dependent on center of gravity of the vehicle. CG shifts towards outer side if vehicle is making a turn, and CG is also shifted fore and aft while vehicle is accelerating or decelerating. Track tension acting with suspension spring, tends to lift the outer wheels and creating more loads on inner wheels. For constant speed there is no inertia tension, and the peak inertia tension is observed when the track slips, but this force is reaction to applied traction and no new force is introduced in the system. Inertial tension is estimated as 20.6 KN. A peak deceleration of 5 square meter is observed for which traction force is calculated as 30.5 KN at combat weight by Newton's

second law of motion. Adding this with inertia tension, total traction is 51.1 KN which is less than peak track tension, which does not produce a governing load case for track design. Therefore, it is concluded that inertia forces are not significant. Vibration is created due to the difference between pitch radius and minimum radius of the sprocket wheel. Considering the peak speed of 18 m/s, the sprockets strike the track with a frequency of 125 Hz, i.e. after every 0.008 seconds.

A case of armored vehicle negotiating the obstacle and a case of vehicle turn is considered to analyze uneven ground conditions. A stress analysis is considered for pins, rubber bushes and shoes of the track. The case of vehicle turning while crossing obstacle is observed as critical loading case. Keays [9] considered a simple sharp edge concrete kerb as obstacle, in this case the author opines that all weight of one side of the track will be carried by the obstacle and the concrete kerb will be destroyed. A less severe case is while vehicle crosses a slope because vehicle loading is not supplemented by centripetal force. In these cases of uneven ground conditions, bending of track shoes produces extraordinary stresses which are in excess of the ultimate strength of the proposed substitute material. In the end, the author suggested that a silicon carbon whisker-reinforced metal matrix composite may have sufficient strength for use as substitute material, although design and development of such a track will have its own difficulties.

### **2.1.3 Thermographic Scanning of Track Pads**

Elastomer track pads are used because it subsides vibrations and noise which is much wanted requirement for military masterpiece. Pergantis [3] used the technique of thermography to carry out thermal screening of track pads. He used Inframetrics Model 600 infrared scanning radiometer within 8-12 micron spectral bandwidth and a video camcorder (8mm) during his experiment. Elastomer track pads gets worn out with time and therefore have limited life which costs the armies heavily due to replacement requirements. Understanding the techniques to better estimate the lifetime of track pads has significance. In his work, the author identified three major failures (a) abrasion (b) cutting and chunking (c) blow out. Author concluded that the failure is attributed to high temperatures encountered by rubber pads, he also used the thermal probes to measure the experimental temperatures experienced by track pads. Three types of experimental comparisons are made by the author which includes effects due to asymmetric loading, pad configuration and material configuration, all these will be discussed sequentially.



In his work, he analyzed the temperature difference of both tracks due to asymmetric loading, he concluded that the right track has more temperatures than left track due to natural asymmetric weight of the tank. The CG of the tank lies more towards the right track and causes the right track to be hotter by 8°C. The author also compared two types of pad configurations chevron and full area pad configuration but his focus is only the ground side surface of the pad. The author concluded that the chevron style pads produce more heat than full area pad and the area that comes in contact with the road wheels received more loads and yields higher hysteretic stresses. This road wheel effect is not observed in full area pads configuration due to increased surface area and thickness of the pad. Driven and trailing bushing regions were also evaluated. Driven bush faced more load than trailing edge bush due to sudden impact of road wheel and produced more temperatures. While driven over idler wheel and sprocket, greater torsional stresses are produced in the bushings. A natural weakness in this experiment is found to be the non-availability of data for trailing bushing's temperature in full area pad design because trailing bush is obscure with pad area. In general, full area pad showed lower thermal profile than chevron style pads. Another aspect of testing was material comparison, in this work various materials were tested but the author mentioned only few. SBR and Triblend materials showed similar behavior. Fiber filled materials were also tested and these materials despite having higher stiffness showed higher temperatures, the possible reason the author opined for this contradiction is poor interfacial bonding between rubber and fiber. The author also tested a proprietary material whose name and composition is not disclosed and the author concluded that this material showed lightest temperatures.

#### **2.1.4 Exploring the Meta-materials**

M1 Abrams tanks are employed by US Army which uses track pads (T158LL) to provide better and smooth traction with sound dampening, and to protect the road surfaces [10]. Styrene-Butadiene Rubber (SBR), filled with carbon black is used as material of these pads, this carbon black reinforcement is used to improve pad's overall strength and abrasion resistance [11].

Due to high-speed operations, the trackpad experiences failures, through blowouts. The rapid cyclic compressive loading or fatigue causes overheating and hysteretic losses, which eventually increases temperature in the range of more than 300°C [12]. Pergantis [3] also identified three major failures discussed above, and attributed these failures to high temperatures encountered by rubber pads, all this causes pads to break apart and deteriorate. Despite the fact that rubber is relatively inexpensive, current manufacturers explain that in order to replace the damaged rubber part, complete assembly be removed and discarded. This

increases the cost associated with this repair, as steel linkages are more expensive [11]. This provides a motivation and opens up a research area to replace elastomer pads by some new material by which hysteretic losses be eliminated or reduced [8]. A metamaterial is the answer to this new pathway.

Initial attempts to design a cellular structures are carried out by Satterfield [5] and Kulkarni [6] which covers conceptualization of unit cell and some experimental and numerical testing to carry out proof of concept. The initial work revolves around obtaining the meta-material from unit cell synthesis and modified unit cell synthesis. These unit cells are tessellated to form a representative volume element (RVE). Optimization is then performed to curve match the desired non-linear response. Franklin [8] in his work, took a deeper dive to prove whether these meta-materials can be used as other non-linear applications or not.

#### **2.1.4.1 UCS**

UC synthesis can be considered as the beginner work for design of metamaterials with targeted material properties [5]. A material tensor which comprises many components, can define nonlinear behavior of deformation of a metamaterial. Satterfield opine that only one or two (for that matter few dominant) modes of deformation are sufficient to define nonlinear behavior of target metamaterial.

Satterfield [5] work is focused on achieving a metamaterial from unit cell synthesis method for use as alternate to elastomer track pad of M1 Abrams. Initially a fixed-fixed beam (zeroth order) design is considered but found infeasible. Then oval beam and fixed-fixed beam are combined in a duo design, size optimization is performed and a metamaterial is obtained which showed compliance to targeted nonlinear deformation but, the stresses obtained surpassed the yield strength of constitutive material (steel) by 400%, which renders physical implementation impossible for use as trackpad. A so called “meta-strain” is also defined by the author as the percentage of the “bulk” uniaxial deformation, i.e. averaged displacement, of the RVE (meta-material).

#### **2.1.4.2 MUCS**

In view of the shortcomings of the current method, Kulkarni proposed a modification [6]. He introduces a multi-objective optimization set-up which is a step in the direction of automating the entire metamaterial design process. The new method that is modified unit cell synthesis method, is utilized to replace the elastomer trackpad by new metamaterial. The author deduced that there are two important requirements which should be considered while designing

metamaterial. The one is to know the overall dimensions of the metamaterial structure which is to be produced and the target response behavior of the metamaterial that is to be used for replacement of elastomer backer pads.

Kulkarni [6] considered the compression as predominant mode of deformation of the backer pad in static loading case and sets the target to achieve nonlinear behavior of meta-material under compression on same lines as the elastomer in use. The author considered the metamaterial design should have 20% maximum compressive strain, but at loads corresponding to 30% strain, the material behavior resembles elastomer behavior.

Unit Cell Synthesis method can be applied keeping these design requirements in mind. A cantilever beam (CB) is selected as a design choice because it offers increased stiffening behavior over fixed-fixed beam (FFB). A cantilever beam geometry is initially conceptualized but satisfactory results are not obtained then a higher order configuration is adopted. Finally, an oval beam is added in series with the existing cantilever beam to construct the new UC.

A material with lower ratio of Young's modulus to yield strength ( $E: \sigma_y$ ) is considered best for track pad applications [13]. Higher the Young's modulus, higher the stiffening behavior of material and lesser deformation will take place. Thus a lower ratio of ( $E: \sigma_y$ ) is best suited when larger deformations are required. A grade of titanium alloy (Ti 3Al-8V-6Cr-4Mo-4Zr-0.05Pd) having ratio  $E: \sigma_y = 92.5: 1$  with material properties ( $E = 102$  GPa, yield strength = 1103 MPa and Poisson ratio of 0.3) is identified as an ideal constitutive elastic material for the metamaterial track pad.

Metamaterial has been designed using targeted nonlinear behavior under static loading case that is compression only but in dynamic loading a tank track pad undergoes compressive and shearing loadings which is evaluated using metamaterial just designed by unit cell synthesis. A comparison of dynamic loading with elastomer track pad and metamaterial is also important.

A model with three track link is created using elastomer track pad and another model with metamaterial central backer pad. A beam element is used between each sub assembly to establish a connection between track links. The model is placed on flat rigid surface. The steel road wheel ( $E = 210$  GPa,  $\nu = 0.3$ ,  $\rho = 7850$  kg/m<sup>3</sup>) is layered with rubber layer (material properties are not known) of 0.0254m thickness. A second order Ogden hyperelastic model is used for elastomer backer and ground pads, and for the rubber layer around the road wheel. Track tension and compression both are required to be simulated: track tension is simulated by

applying lateral force of 22500 N in one direction at the end of beam connector (rigid beam) and keeping the opposite beam connector constrained with respect to all DOFs.

A tie constraint is used between steel plate and ground pad and backer pad and steel plate, this constraint ties two separate surfaces together in Abaqus [14]. A rigid body constraint is used to constrain the motion of the road wheel with respect to the motion of a reference point which is center of the road wheel. This helps in saving the computational costs as road wheel analysis is not necessary in this case. Secondly, the material properties of the rubber layer at the wheel periphery are not known which can create numerical errors. Tank weighs 63 tons, thus the load calculated for each pad is 22500 N, tank speed is assumed to be 40 mph and linear and angular velocities are calculated and applied to the wheel. The wheel roll over event is created under its weight, to capture the deformation response in the pads. Penalty formulation with friction co-efficient of 0.4 is chosen to define the tangential behavior.

The nonlinear dynamic finite element analysis is run for a time period of 0.026 seconds. In the first simulation, all three backer pads are modeled with the elastomer material properties. While in the second simulation, only the central backer pad is replaced by the Canti-Oval metamaterial.

Central backer pad represents the actual real conditions which are experienced by track pads and thus selected for analysis. The displacement in y-dimension is compared for both type of analysis at three different locations on the backer pads. The elastomer undergoes a maximum deformation when the road wheel is directly above it. For all three locations, metamaterial shows lower deformation when compared to the elastomer. When the road wheel moves from left to right the deformation error value increases, with average error within 7%. Kulkarni [6] attributes this deformation error to the reason that the meta-material is designed with dominant role of compression but, in actual the backer pad experiences both shear and compression which causes variance. The author concluded that metamaterial track pads can indeed be used as replacement of elastomer track pads. As a future work, Kulkarni [6] suggested: to carry out stress reduction with different UC designs of metamaterials; fatigue analysis to estimate the life of metamaterial and author recommends 400,000 loading cycles as a target for fatigue life; and a detailed 3D analysis can be performed to simulate the actual road wheel and track pad interaction.

### **2.1.4.3 Design of Meta-Materials with Targeted Nonlinear Deformation Response**

Satterfield et al. presented [7] the design of metamaterials from unit cells. Metamaterials are used to achieve desired global properties which are different from the one of their constitutive material [15]. The authors highlighted three popular methods for designing metamaterials which includes computational methods (size/shape and topology optimization) and synthesis method. Synthesis method serves as alternate to other optimization methods mentioned above. The authors in their research have used unit cell synthesis method but the scope is limited to 2D geometries only.

Satterfield et al. [7] considered a military track pad as a case study. M1 Abrams tanks are employed by US Army which uses track pads (T158LL) to provide better and smooth traction with sound dampening, and to protect the road surfaces [10]. The material used is SBR filled with carbon black, addition of carbon black reinforcements helps improving strength and abrasion properties of these pads [11]. Trackpad undergoes cyclic loading (fatigue) due to high speed sustained operation. This can cause temperatures exceeding 300°C due to friction and hysteretic losses [12]. Cost of repair and replacement of trackpads is also very high. Elastomer rubber pads do have desired compliance for sound dampening and traction but these rubbers are viscoelastic in nature and produces hysteretic loss, producing higher strains at low stress levels. Solution to this problem lies in designing a metamaterial which should contain elastic material and are inherently non hysteretic. Thus hysteretic losses do not pose significant problem when the material is designed with linear elastic base. Target strain values are calculated by the authors for the potential design of metamaterial. A maximum of 20% strain is worked out by Dangeti [16] in another work.

Satterfield et al. [7] have discussed three types of EFGs (Elemental Functional Geometries) which includes cantilever beams (CB), fixed-fixed beam (FFB) and oval structures. FEM is used to define large scale deformation. Unit cell synthesis method makes a systematic development of structures which uses simple EFGs to design a global deformation non linearity. The authors considered three materials which can serve as constitutive materials namely steel, aluminum and titanium alloys. Brick oval and CB designs are considered infeasible because of higher elemental stresses under a 20% target strain. The authors concluded that the Canti-Oval design is a feasible design using titanium alloy as constitutive material. Fatigue analysis is not considered by the authors, and they suggested that more EFGs (cross shaped, L shaped and variable thickness) can be considered for future work.

#### **2.1.4.4 Design of Meta-Materials Backer pads with Additive Manufacturing**

The initial steps in obtaining cellular materials, revolve around the unit cell design, have been discussed in previous sub sections. These UCs constructed of elemental functional geometries (EFGs) and elemental support geometries (ESGs), which act as building block. Tessellation of these UCs is carried out and RVE is formed. These RVEs are of two types: one is where size of global structure is much larger than base UC, this is suited when boundary conditions are not known; the other one is the RVE comprising small number of UCs in x and y directions. Beam elements placed in different combinations of series and parallel arrangements produce a general pattern of cellular material. Three cell configurations are considered as candidate options and explored to check feasibility for multi-objective optimization. In first configuration, two cantilever beams are combined to form a ‘Canti Duo’, this is considered as simplest configuration by the author. In second configuration, a cantilever beam is combined with an oval beam in parallel and is given the name ‘Canti-Oval bi parallel’. In third configuration, cantilever beams and oval beams are combined in series instead of parallel, this configuration is named as ‘Canti-Oval’. All these are connected to ESG (elemental support geometries) at the other end.

Dimensional optimization is then performed to curve match the desired targeted response. A multi-level optimization objective function is chosen with two design objectives: the first is to minimize the sum of the squares of the errors between the target and predicted strains; and the second is to minimize the maximum stress. The NSGA-II search algorithm is applied to search the design space which evaluated up to 1000 possible solutions. Optimization results showed that the third configuration ‘Canti-Oval’ has 65% feasible points and considered as most optimal choice. This design boasts lowest stress and strain error amongst all three configurations. Physical parts are printed through additive manufacturing and mechanical behavior of these printed parts is analyzed through fatigue and compressive testing. Franklin [8] in this study is looking to conclude whether metamaterials can be used to replace elastomer trackpads, and also investigating whether these materials can be used to replace the other rubber components. In this study, results of FE model and physical (experimental) behavior of titanium pads is compared. Franklin [8] considered original material FE analyses with a maximum load of 4 MPa but due to testing limitations, loading is kept at 1 MPa of pressure, or 22.5 kN (static loading) across the pad’s top surface. A nonlinear deformation response is observed as the material shows stiffening as the load increases.

Both tests are run and discrepancies are observed in results of numerical simulations and experimental results. Compressive testing (static loading case) experimental results showed the behavior of pad is approximately 2.5 times softer than expected. Fatigue test for 400,000 cycles was considered (for a 500 miles run) as it was estimated by Kulkarni [6] and already discussed. This test was important to understand the reliability of metamaterial. It was initially expected that the metamaterial would meet the 400,000 cyclic loading requirement but the pad experienced critical failures only after 8000 cycles which are identified in ANSYS model by Franklin. It does not come as a surprise because in static loading response is already found deviating from original FE model. Since fatigue is also cyclic compression so it also behaved in the same way and showed major deviations from expected life.

Three potential reasons are identified for these deviations and the author believed that all this contributes to these causation: one is that the assigned material properties which are provided by manufacturer may not be actual; EBM (electron beam melting) process printing tolerances; loading and boundary conditions used may be different from the one experienced by pads.

Franklin [7] used MUCS methodology to design a circular layered meta-material for the rubber-rubber track system in order to explore whether full system design is possible with meta-material or otherwise. The author concluded that additional applications of meta-material particularly in non-linear domain are an achievable goal. The next step is optimization, as to which of the two, single level or multi-level optimization is the better choice with respect to final design, computational efficiency and convergence accuracy. The author concluded that single level optimization is better choice for design aspects and author is unable to decide any conclusion for convergence accuracy because multi-level optimization algorithm was terminated before global iteration limit of 10 loops is met.

### **2.1.5 Terramechanics Models**

In another work [17], modeling of steady state performance of skid steering is carried out for tracked vehicles by Tang et al. Their work describes a high-fidelity, general, and modular method for lateral dynamic simulation of high-speed tracked vehicle. Their work used terramechanics to derive a nonlinear track-terrain model. They covered both the scenarios of steady state steering and longitudinal motion.

Previously Wong and Chiang [18] only derived the model which does not work for longitudinal motion. They developed a theory for skid steering under steady state conditions on firm ground and verified with already available experimental data. They developed a relationship for shear

stress and shear deformation for track to ground interaction  $T = T_{\max}(1 - e^{-j/k})$ , where  $k$  is the shear deformation modulus and represents corresponding maximum shear deformation against maximum shear stress ( $T_{\max}$ ). Steering behavior is found in close agreement with experimental data. The authors also concluded that lateral coefficient of friction which is used to calculate the moment of turning resistance can also be derived using their presented theory and hence conventional field tests can be done away with. This theory provides a unified approach for study of skid steering mechanics and it can further be used for study of transient handling behavior of armored tracked vehicles.

Model of Tang et al. [17] includes comprehensive track slips and modular modelling for tracked vehicles. Their model is verified by data made available by experiments of Rui et al. [19]. Their model provides governing equations for traction forces (both lateral and longitudinal) and moment at a point on the track, under normal pressure distribution. Their model also calculates the track motions input which are utilized for dynamic analysis.

### **2.1.6 Tracked Vehicle Model (FEM)**

Model developed by Campanelli and Shabana [13] is believed to be complex but it can be counted as initial work, their work uses FEM and carries out vibration and dynamic stress analysis using ANSYS. The authors claimed that all previous works calculates static stress analysis on the track link, their work carries out dynamic stress analysis with modal forces. Nonlinear equations of motions are linearized basing on the assumption that elastic deformation of track link does not have significant effects on overall track motion. These partially linearized differential equations are used by authors to calculate the contact, inertia, and constraint forces. The finite element method is used to determine the deformations of the track links. The results of the dynamic stress analysis of the track links are presented and the differences between these results and the results obtained by using the static stress analysis are demonstrated. Modal analysis is carried out experimentally by using impact hammer and multi input single output (MISO) measurements. Experimental modal frequencies are also compared with modal analysis performed on ANSYS (both as lumped mass approach and consistent mass approach). The first six mode shapes are depicted; the first mode is identified as torsional mode while the second mode is identified as bending mode.

Another problem of track link modeling is addressed in work of Ryu et al. [20], a compliant track link model is developed, they used rubber bushing single and double pin track links. Mathematical model is developed for both types of track links. Contact forces are established



between all types of contacts with tracks which includes four types of track link and road wheel interactions, four types of track center guide and road wheel interactions, sprocket drive and track link interaction and finally the ground and track shoe interactions. Four main simulation scenarios are presented in the study which includes braking, acceleration, high speed motion and turning. Same angular velocities of right and left track sprockets are used for simulating straight line motion. Numerical simulation with variable step size is used to obtain the results. The authors concluded that bushing stiffness has significant effect on dynamic response of tracked vehicle. Numerical results showed that the bushing forces in double pin model are lesser than single pin model.

Another problem of computing the contact forces is discussed by Lee [21]. A numerical method is used for dynamic analysis of tracked vehicles of high mobility, low mobility tracked vehicles are not considered. Impulsive dynamic contact forces are computed, these forces are generated when a vehicle passes over a ground obstacle. Track links are modeled considering them as elastic links interconnected by pin joints. The mass of each track link, the elastic elongation due to track tension, and the elastic spring effects of each track link are catered in the equations of motion. The road wheels, torsion bar arms and chassis are taken as the rigid multibodies in the dynamic model, these multibodies are connected with kinematic constraints. Modeled equations of motions are solved to compute contact forces and contact positions between the road wheels and track, and between the ground and track. The iterative scheme for the solution of the multibody dynamics of the tracked vehicle is presented and the numerical simulations are conducted.

Easier models are developed by Nabaglo et al. [22] using MSC.ADAMS. This paper describes steps of model construction of a tracked vehicle. A high fidelity model is developed and dynamic simulation is performed at a speed of 22 km/hr. First wheel on the right side is simulated for crossing a rectangular beam and it is shown that vertical displacements of successive wheels are also dependent on first wheel vertical displacement however the successive displacements kept on reducing.

In another work of Nabaglo et al. [23], the authors introduced a new concept of hyperbolic torsion spring modeled by using finite element method. Their work is latest in its domain and can have dividends for the industry of armored tracked vehicles. Armored fighting vehicles uses 2S1 platform and their suspension is mounted on torsion bars. These torsion bars occupy the whole bed of the vehicle and becomes very harmful for the crew in case of a hull explosion in military operations. The problem is to remove these torsion bars and redesign suspension

system using alternate means. The objective is to bring suspension system on the sides and multiple solutions were offered by various authors which need not to be discussed here, however, Nabaglo et al. used all these works as a guideline to produce their latest work. They introduced the use of hyperbolic springs and carried out modeling of these springs using FEM built by using ADAMS and MSC.MARC. They designed these suspension springs using ADAMS software and performed the dynamic analysis of track vehicle.

Nabaglo et al. [23] in their work, also developed full vehicle model by both using torsion bars and removing the torsion bars and placing torsional springs. Contact forces are assumed between track link and wheels, and also between ground and track links. They also assumed contact forces to be linear, other parameters are stiffness and damping between both contact surfaces. They also simulated the dynamic model with one track single obstacle crossing. Their work is focused on suspension system, their vehicle model although latest but does not involve any analysis for stresses on track. The authors concluded that the removal of torsion bars allow extra allowance for increasing the weight of the armored vehicle which can have high utility for military requirements. This design also provides increased stability and removes axial offset of road wheels and road wheels can now be placed in axial alignment which provides more space between the wheels.

### **2.1.7 Dynamic Forces of Weapon System (FEM)**

The research of Banerjee et al. [24] calculated nonlinear dynamic forces. Their work is focused on dynamic loading on mount of air defense weapon system, a mathematical vibration model is derived for gun recoil mechanism and dynamic loading is simulated using excitation forces (rapid firing with five rounds is simulated), the work is done using MATLAB.

The mathematical vibration model is given by

$$M\ddot{X} + C\dot{X} + KX = F(t)$$

The total transmitted force to mount assembly is estimated by

$$F_T(t) = C\dot{X} + KX$$

Where  $F(t)$  is force on recoil system,  $X$  is induced displacement on recoil system,  $K$  is spring stiffness estimated from spring data,  $C$  is damping of the recoil system,  $M$  is reciprocating mass of the recoil system, and  $F_T$  is transmitted force on ADWS.

Developed finite element model uses 10-node tetrahedral finite element, model is developed in Abaqus 6.13. Model is simulated with transmitted load and body loads. Dynamic analysis is

carried out on mount assembly. Vibration response is calculated and location of stresses is indicated on the mount using eigenvalue analysis. Modification in pivot base is suggested in their paper.

### **2.1.8 Rubber Pad Buffer of a Track Type Bulldozer**

Wang et al. [4] analyzed heat accumulation in a rubber pad of a tracked type bulldozer. In this work, the authors performed structural and thermal analysis which included three cases (a) earthmoving, (b) cutting and bulldozing, and (c) loosening. The heat accumulation remained in the contact region where hysteretic heat is produced. The maximum values of temperature and heat flux remained slightly out of service range for earthmoving case. The maximum values in loosening case were out of range. The values in cutting and bulldozing case were below range. Natural rubber pad was used and material data was validated by uniaxial tensile testing. Mooney-Rivlin model for uniaxial tension was used to define the stress-strain relationship. Mooney-Rivlin constants were obtained from curvefitting of experimental data. Hysteresis testing was also conducted to find the coefficients.

## **2.2 Research Gap**

The work related to static and dynamic loading on tank tracks is identified in the literature survey. Development of metamaterial is also identified for backer track pad. FEM is applied on backer trackpads. Basing on the literature and to the best of our knowledge, it is evident that no work is done for groundside track pad. Identified research gap for this work is as follows: -

- a. Analysis of rubberized ground side track pad using FEM.
- b. Comparison of various rubberized materials using FEM.
- c. Impact on steel track body in case of rubber failure.
- d. Shapes comparison for improvement in design.

In other words, the research questions we plan to investigate and answer are as follows: -

- a. What is the best suited material for ground side track pad for various loadings?
- b. Changing the shape will have significant effects on stresses induced in track or otherwise?

## Chapter 3

### Methodology

#### 3.1 Model Development

The tank weight is the primary source of loading on a track pad. The weight of the tank is transferred to the track through suspension system and road wheels. The arrangement can be seen in Figure 3-1. The analysis is focused on track pad and track link assembly therefore, a single assembly is constructed in solid works for static loading analysis. A wheel roll over event is simulated for dynamic loading analysis and for that purpose, a three pair pad-track link assembly is constructed and modeled in ANSYS [25] for stress analysis.

##### 3.1.1 Dynamic Loading Model

Dynamic loads come into play due to power-train and includes simple traction, frictional, inertial and vibrational loads. For dynamic loadings it is not sufficient to use single assembly model because it is expected that the stresses may differ when road wheels approach and leave the track link. Therefore, a three pair track link assembly is constructed in solid works and depicted in Figure 3-1. Analysis settings and loads will be discussed in subsequent sections.

##### 3.1.2 Static Loading Model

The model depicted in figure 3-1 can be further reduced to a single track pad model for static loading analysis. The static analysis model is depicted in Figure 3-2. This pad-track link assembly contains an elastomer backer pad resting on a steel body and another elastomer pad is fixed on the ground side of the track link. The road wheel rests on the backer pad and transfers tank's weight vertically when resting on the flat rigid surface. The pins are used to connect the track links which works in tandem as depicted in Figure 3-1. Rubber bushes are mounted on the pin to create a cushion within track link and easy slip conditions to reduce the heat.

The vertical load is applied by the road wheel and calculated from tank's weight. The tank weighs 53 tons which is transferred to 12 road wheels. Each road wheel transfers this weight to a pair of track pad assemblies connected in tandem. Thus, the overall weight of the tank is divided by 24 and a weight of 4946 lbm is calculated for single pad assembly. Since weight of the tank is not symmetric for both tracks and a disparity of 30% is highlighted by Pregantis [3], a cushion of 30% is added. Hence, a force of 6500 lbs is applied on the track pad for compressive loading analysis. The pad assembly is put to rest on a concrete floor. The model is developed in ANSYS (Static Structural) [25] and is shown in Figure 3-3.

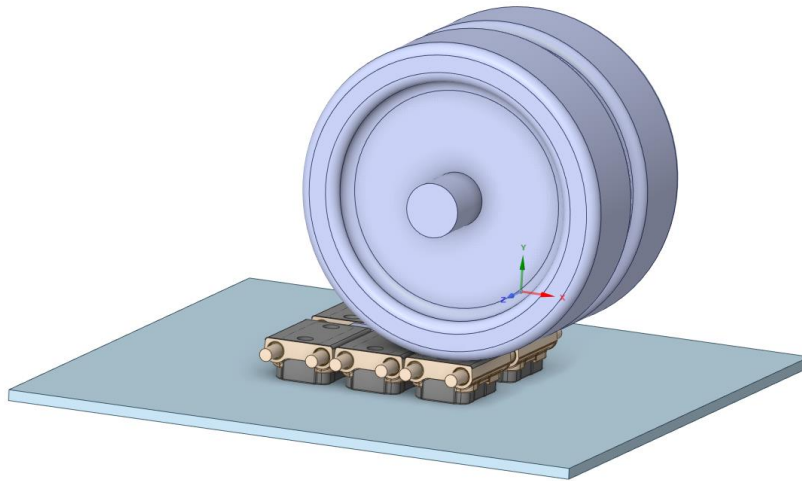


**Figure 3-1: Track Assembly Model**

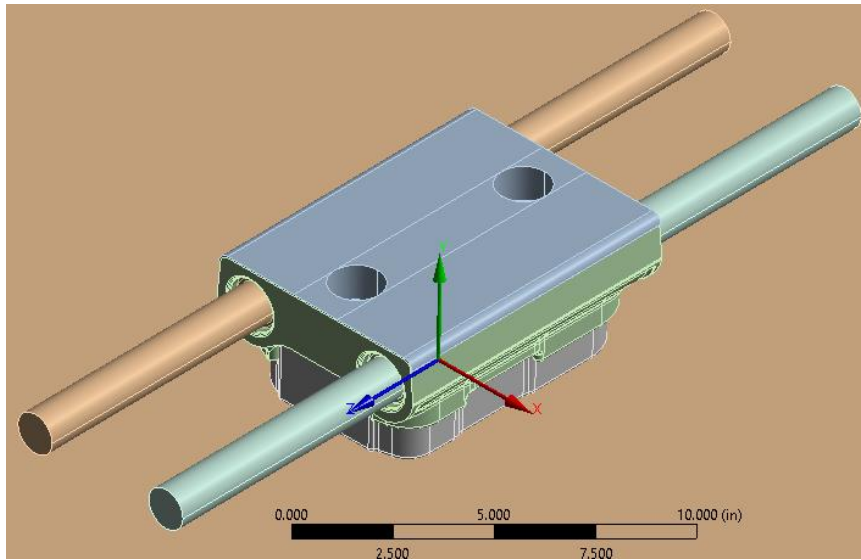


**Figure 3-2: Static Analysis Model**

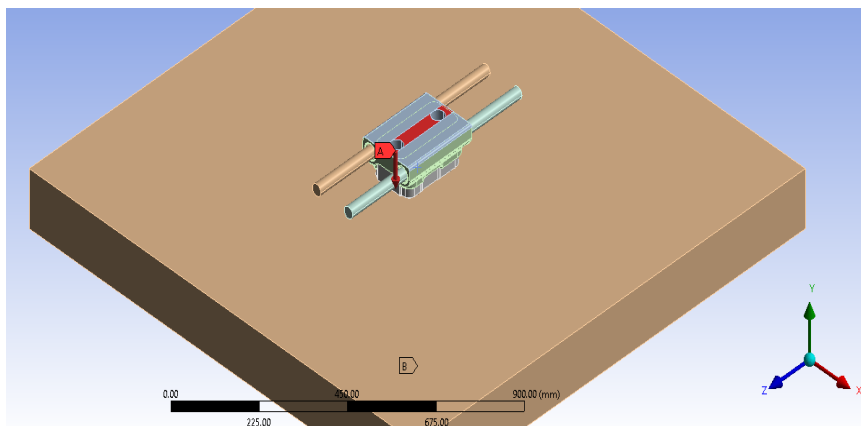


**Figure 3-3: Force & Fixed Support**

## 3.2 Material Selection and Validation of Rubber Material

The next problem faced is to what material these components should have in order to sustain all types of loads. Flat resting floor is modeled as concrete while steel material is fixed as AISI 4140. However, the rubber material is not fixed and a number of materials are being developed in local industry and the analysis is required with all these materials. SBR filled with carbon was used in M1 Abrams is considered for initial setup. A proprietary rubber material is also considered for validation on rubber material through experiment.

### 3.2.1 Experimental Test

A proprietary rubber specimen is tested as per ASTM D-412, material properties are determined as shown in Table 3-1. A stress-strain curve and a force-deformation curve is obtained and are shown in Figures 3-4 and 3-5 respectively. The behavior of the material is nonlinear as expected. The specimen for physical tests is shown in Figure 3-6 and tensile testing is shown in Figure 3-7.

**Table 3-1:** Tested Material Properties of Proprietary Rubber

Density (g/cm <sup>3</sup> )	UTS (psi)	Modulus at 200% (psi)
1.183	2638	1040

### 3.2.2 Modeling in ANSYS

The next problem is to simulate the physical test in ANSYS for validation of technique. Stress-strain data is fed into ANSYS through curve fitting technique. 1<sup>st</sup> order Ogden model is used to define nonlinear material behavior based on this stress-strain data, material coefficients of Ogden model are depicted in Table 3-2. The tensile coupon is shown in Figure 3-8. The coupon is 80 mm in length, 14 mm in height and the height of neck is 3.5 mm. Thickness of the coupon is 6.63 mm. The next step is to model this coupon in ANSYS. CAD model and mesh is created in ANSYS. One end of the model is fixed (fixed support marked as B in ANSYS) and magnitude of force (as per experimental force) is applied at the opposite end to create a tensile simulation, the same is shown in Figure 3-9. Figure 3-10 shows the deformation result at 251.3 N force. The maximum deformation is 106.45 mm at this force. The simulation and experiments are performed at various load steps and both physical and simulated results are found in good agreement with each other. The results at all load steps are shown in Table 3-3. The variation between results is maximum up to 10.7 % which is accepted for this analysis.

The same is shown in Figure 3-5. Hence, it is appropriate to apply this rubber material in our problem.

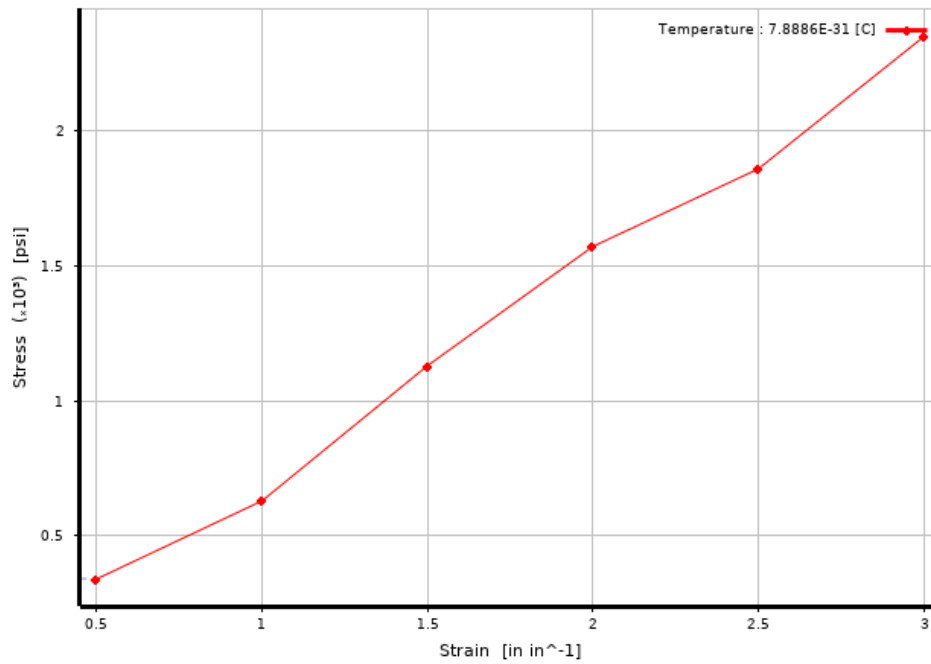


**Figure 3-4: Stress-Strain Curve of Rubber Material**

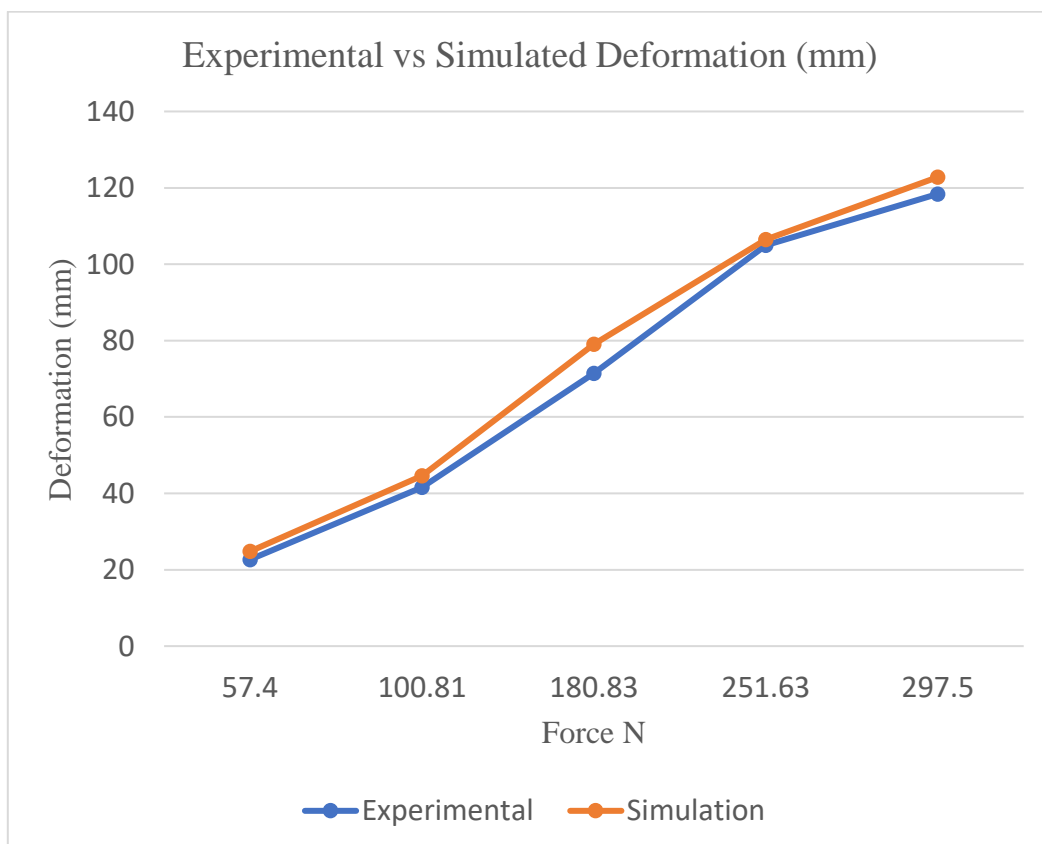


**Figure 3-5: Force-Deformation Curve**



**Figure 3-6:** Rubber Coupon



**Figure 3-7:** Tensile Testing



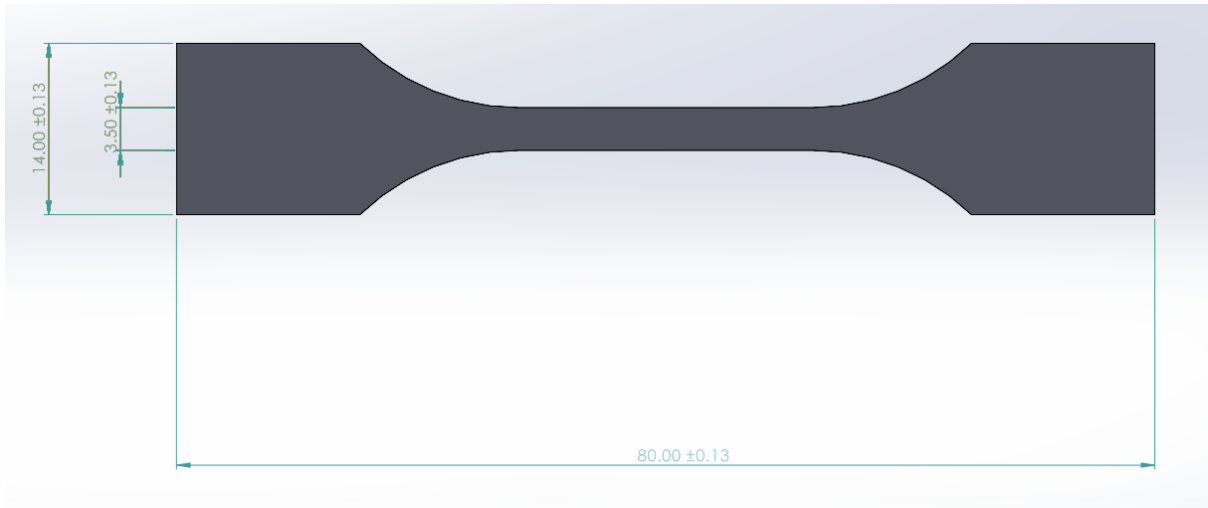


**Figure 3-8:** Coupon Dimensions (mm)

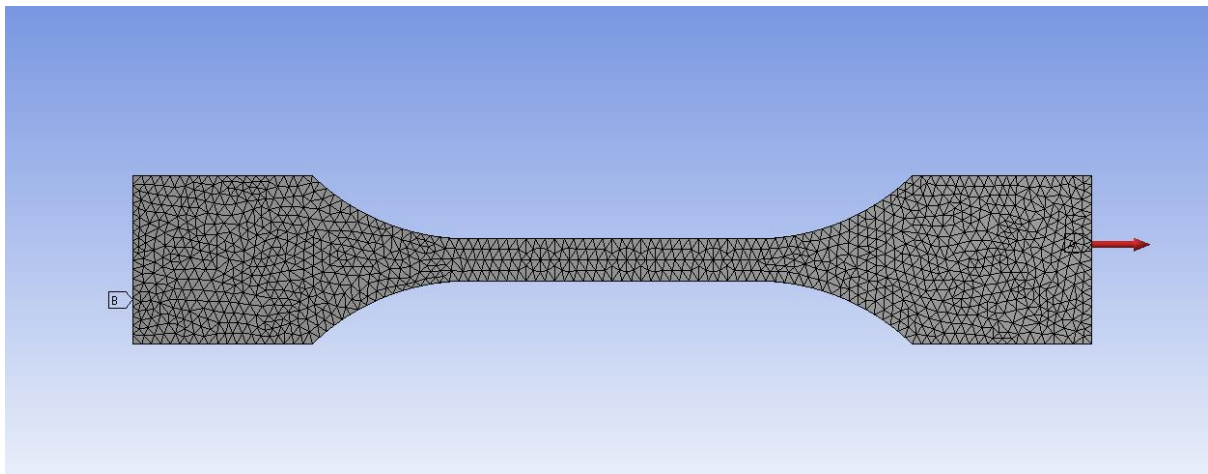


**Figure 3-9:** Tensile Coupon Model in ANSYS

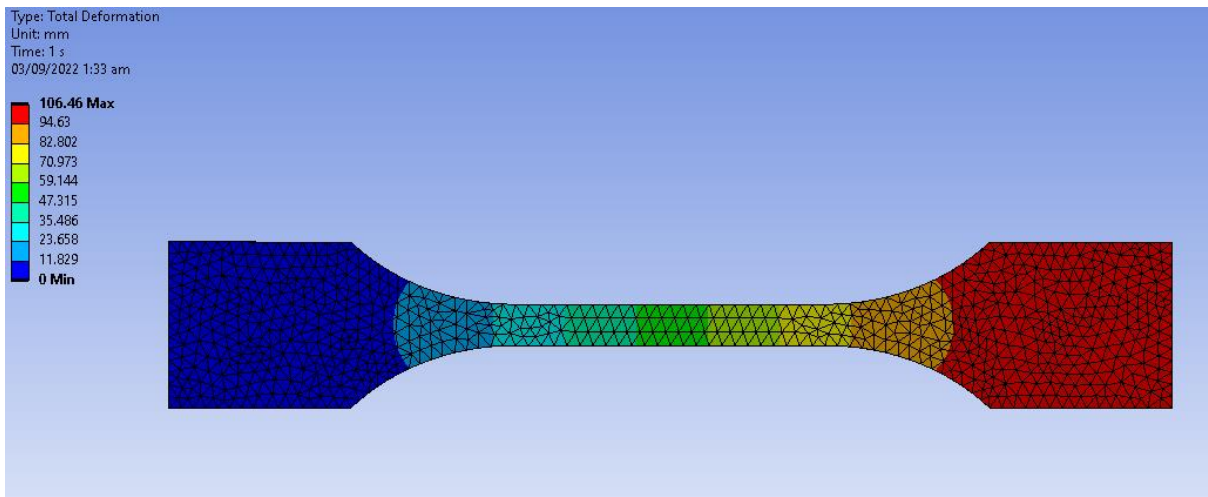


**Figure 3-10:** Deformation Results

**Table 3-2:** 1<sup>st</sup> order Ogden Model Coefficients

<b>Material Constant MU1 (psi)</b>	<b>Material Constant A1</b>	<b>Incompressibility Parameter D1 (psi<sup>-1</sup>)</b>
204.07	2.7926	0

**Table 3-3:** Deformation Variation in Experimental vs Simulation Results

<b>Force (N)</b>	<b>Experimental (mm)</b>	<b>Simulation (mm)</b>	<b>Error (%)</b>
57.4	22.67	24.81	9.4
100.81	41.572	44.60	7.2
180.83	71.395	79.05	10.7
251.63	104.98	106.45	1.4
297.5	118.4	122.8	3.7

### 3.3 Mesh Independence

The model shown in Figure 3-2 is required to be solved. But the model has so many geometries with small and fine surfaces. The question arises what type and size of mesh settings be used to get the acceptable results within available computational resources. Program controlled (linear and quadratic) tetrahedron elements are selected to keep the problem computationally easy. Mesh independence is performed by varying maximum element size, 20% size is changed for each successive solution. Floor is fixed and track is made to rest on the floor and all DOFs are kept free. A compressive force is applied on top of the pad as already discussed in section 3.1.2. The type of contact with rubber is bonded with asymmetric behavior. The results of mesh independence are shown in Figure 3-11 and are subsequently used to develop more models. The points of maximum deformation and maximum strain in the model appears at different locations but strain is considered for mesh independence due to its sensitivity in this model.

The error between two heaviest mesh is 1.15 %. Error at all sizes are shown in Table 3-4. The selected mesh has 1,270,549 number of elements, 1,983,490 number of nodes and maximum strain value is equal to 1.9514.

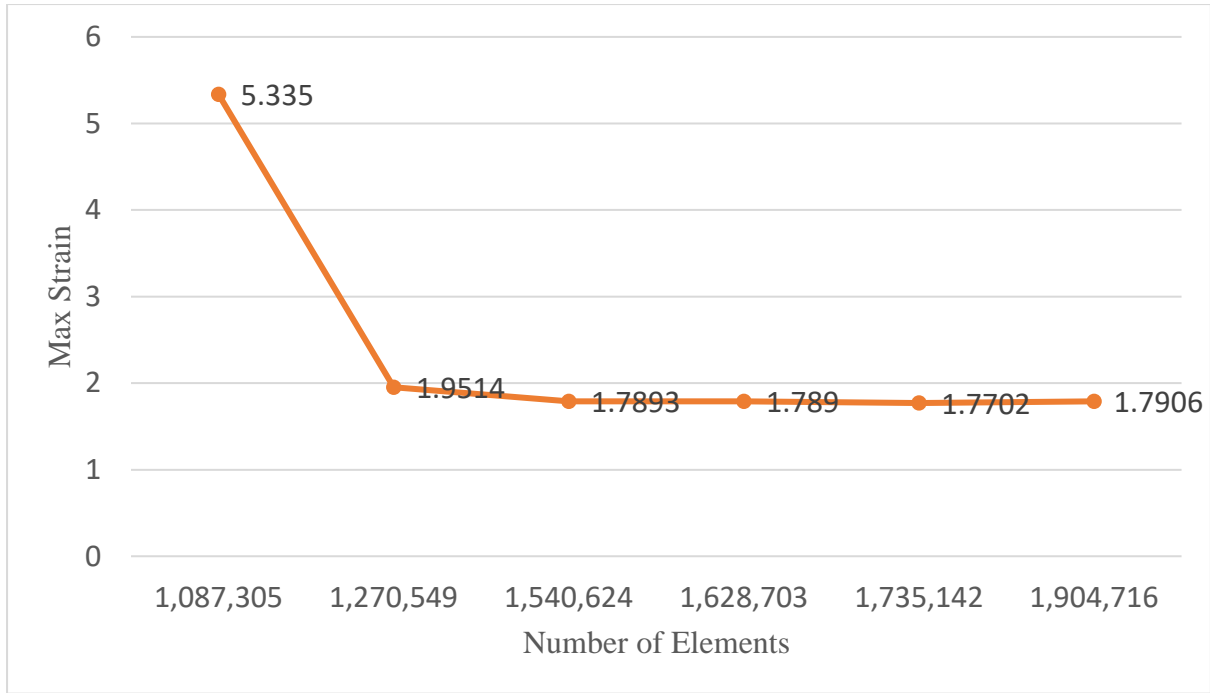


**Figure 3-11: Mesh Independence**

**Table 3-4: Mesh Independence Error**

Number of Elements	Strain value	Number of Elements	Strain value	Error (%)
1,904,716	1.7906	1,735,142	1.7702	1.15
1,735,142	1.7702	1,628,703	1.789	1.06
1,628,703	1.789	1,540,624	1.7893	0.01
1,540,624	1.7893	1,270,549	1.9514	9.05
1,270,549	1.9514	1,087,305	5.335	173

## Chapter 4

### FEA Results

#### 4.1 Materials Comparison at Static Loads and Varying Loads

Focus of this research is not on material formulations as to how they are composed chemically. Though a few materials have been considered for comparison to find the best performers. It is hoped that some local industry material may outperform the original proprietary rubber.

A variety of rubber materials are available in ANSYS for analysis, most of these materials are nonlinear. A few are considered appropriate for use in track pads, namely butyl rubber, neoprene rubber, rubber nitrile (NBR), Polyurethane, SBR, and natural rubber. A few are shortlisted for further analysis.

##### 4.1.1 Material Comparison as per ASTM D-412

A material comparison is performed for rubber material on ASTM D-412 model shown in Figure 3-9. SBR filled with carbon black, butyl rubber filled with carbon black, non-linear natural rubber and nonlinear proprietary rubber are used for comparison.

Load vs deformation curve, load vs factor of safety curve and stress vs strain curve are plotted and comparative results are displayed in Figures 4-1, 4-2 and 4-3 respectively. SBR and Butyl rubber formulation fails at 40 N force in this numerical simulation therefore it is not included for further discussion in this particular case. Natural rubber formulation shows softer behavior (larger deformations) than imported proprietary rubber and this softer behavior of natural rubber formulation is enhanced at higher loads. Natural and proprietary rubber materials considered in this analysis are nonlinear. The nonlinearity is not clear in Figure 4-1 but on close examination of values, the nonlinearity is seen. This nonlinearity is clearly visible in Figure 4-3. If we closely observe the curves in Figures 4-1 and 4-3, we find that for a particular load step corresponding to some particular strain the nonlinearity can be ignored and value of modulus at that point can be used for defining the material in ANSYS. Stress strain curve in Figure 4-3 also shows that the behavior is linear at small loads. At this point we consider it important to discuss the factor of safety. In engineering problems, the factor of safety is a measure of strength that a particular system is intended to display for given loads and conditions. Mathematically we can write: -

$$FoS = \frac{Yield\ Stress}{Maximum\ Stress\ in\ the\ system}$$

Figure 4-2 shows that factor of safety of natural and proprietary rubber formulations are well within the safe region and behaves almost similar at higher loads.

**Table 4-1:** Material Properties of Shortlisted Materials

Name of Material	Density (g/cm <sup>3</sup> )	Young's Modulus (psi)	Poisson's Ratio	Tensile Ultimate Strength (psi)
SBR filled with Carbon black	1.14	692.56	0.4879	2958.8
Butyl Rubber filled with Carbon black	1.158	813.95	0.4992	1236.3
Natural Rubber Proprietary	1.175	670	0.49	3340
Rubber Proprietary	1.183	1040	0.49	2638

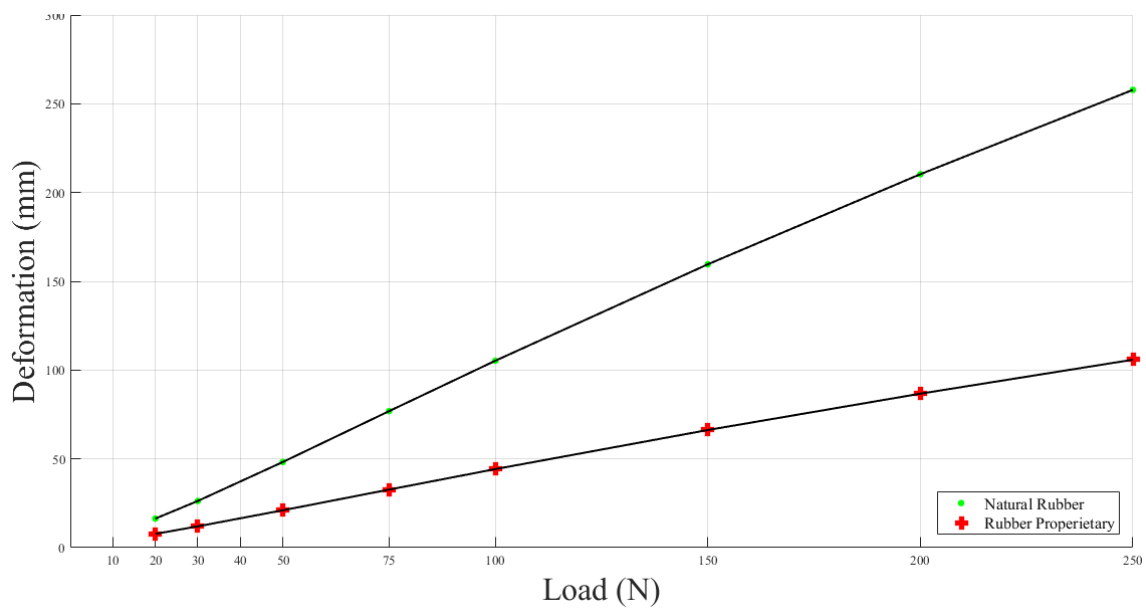


**Figure 4-1:** Material Comparison at Varying Loads (Load vs Deformation) –ASTM D-412

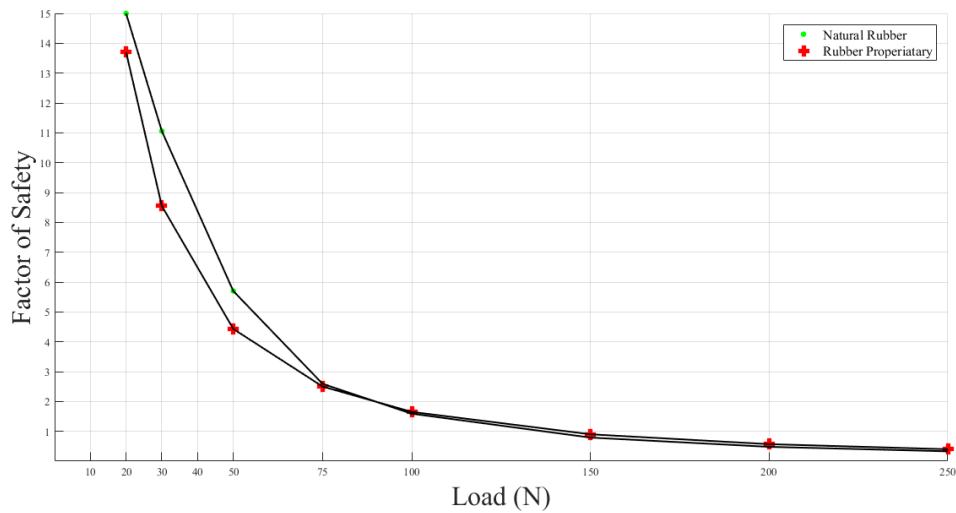


**Figure 4-2:** Material Comparison at Varying Loads (Load vs FoS) ASTM D-412

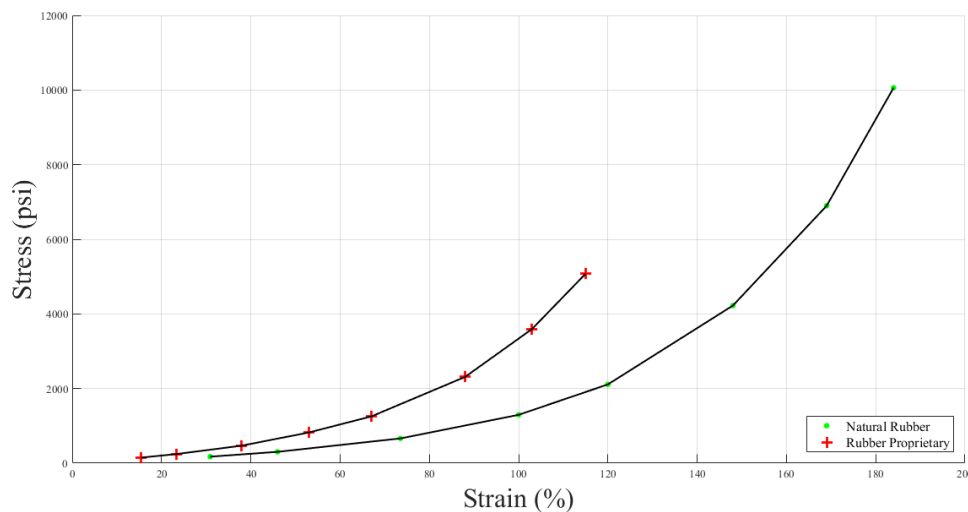


**Figure 4-3:** Material Comparison at Varying Loads (Stress vs Strain) ASTM D-412

#### 4.1.2 Material Comparison on Static Loading Model

Many of the rubber materials are inherently nonlinear and attempts are made to solve the model with nonlinear materials but the model is complicated and computational resources are limited. As a consequence, the nonlinear materials discussed above are linearized at 200% modulus (the value is obtained from experimental data) and used for further analysis.

Overall four types of formulations for use in groundside rubber pads are shortlisted for analysis in this work. Table 4-1 shows material properties of four shortlisted rubber materials. Model under evaluation is already shown in Figure 3-2 for static loads. SBR is used for bushes and

AISI 4140 (being indigenously developed) is used for metallic track body and track pins. SBR, Butyl, a locally produced natural and imported proprietary rubber formulations are used in backer pad and groundside pad for comparison. Model simulated at four different loads, 1<sup>st</sup> load step is equivalent to static compressive load (6500 lbf). Comparative results are plotted and displayed in Figures 4-4 and 4-5. A further analysis is also performed by changing steel from AISI 4140 to structural steel and results remain almost similar.

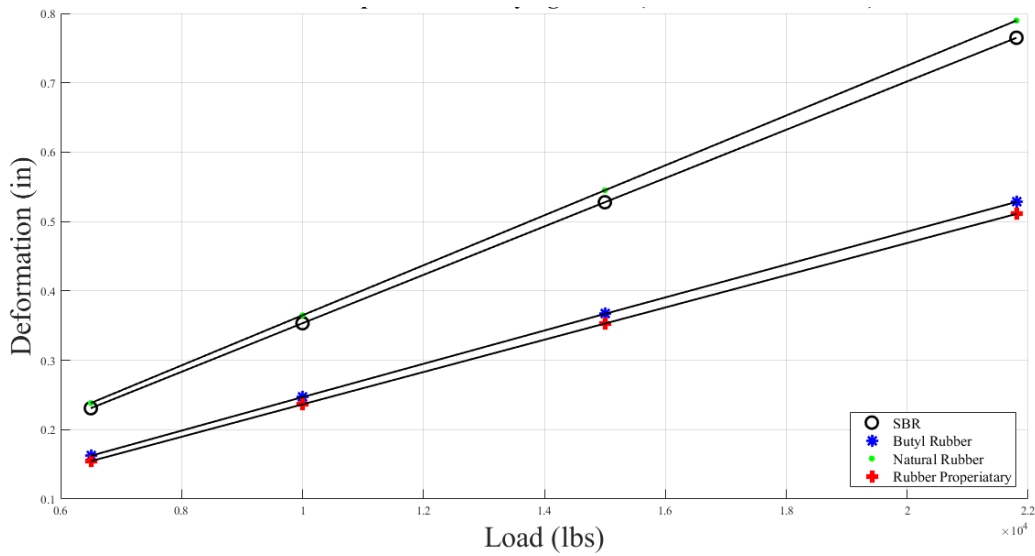


**Figure 4-4: Material Comparison at Varying Loads (Load vs Deformation)**

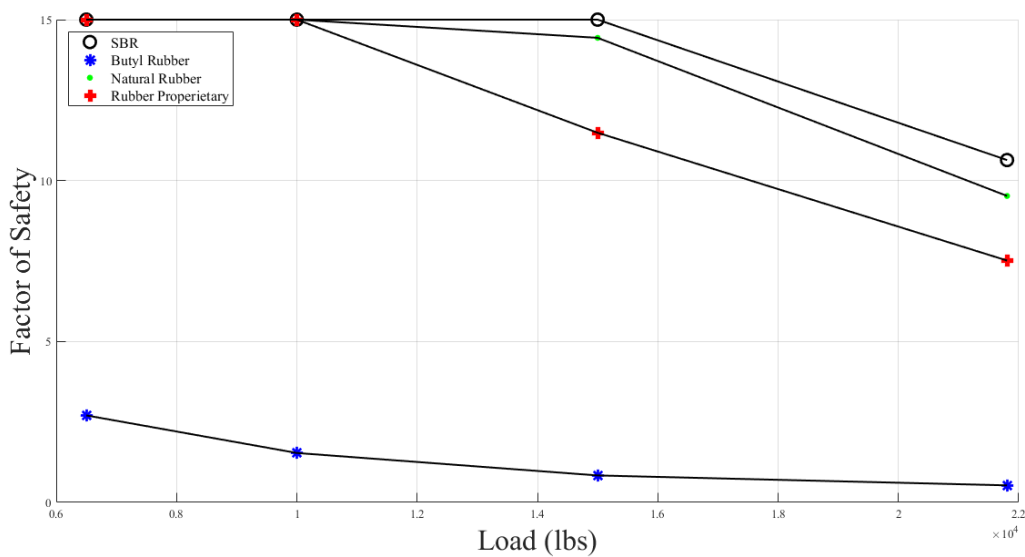


**Figure 4-5: Material Comparison at Varying Loads (Load vs FoS)**

## **4.2 Shape Comparison**

In this section, we address the second research question “Changing the shape will have significant effects on stresses induced in track or otherwise?” To answer this question, first the ground side of the original track pad design is studied. The original ground side pad and general pattern of stress distribution is shown in Figure 4-6. Load is applied on the center strip from the opposite side. Stresses on the shorter dimension (x-axis) are more in comparison to the larger dimension (z -axis). The behavior is symmetric about the center.

There is a possibility to change the shape and get better stress distribution. Changing track width is a major design change which will require change in overall suspension and road wheel dimensions. Since track width cannot be changed much and the new variant must confine to general dimensions of original track. Options available within the same dimensions include reduction in thickness, addition in thickness, introduction of sub-patterns within the same shape and changing the pattern altogether. In this research, five new sub-patterns are introduced. Volume reduction is performed in four patterns by making cuts within the ground pad from ground side. Volume is added in one sub-pattern. One new shape is designed inspired from chevron style but overall dimension is kept almost the same as original. The contact area of pad with ground has become a variable and it may have some impact on stress distribution and stress reduction. The volume of the pad has also become a variable and its impact is also required to be analyzed. Overall six shape variants are compared with original design. The material choice is made based on previous section results and kept same in this analysis, these are discussed in detail in subsequent chapter.

### **4.2.1 Original Pad Design**

The model for groundside as developed using simulation software is shown in Figure 4-6. The analysis is focused on ground pad and more specifically on the groundside of the ground pad. The analysis setting is already explained in previous sections. The stress results at groundside and overall maximum stress on the pad are shown in Figures 4-7 and 4-8 respectively. The results obtained depicts that the maximum stress on the pad lies on the surface that is bonded with steel body with the value 826.88 psi. The maximum groundside stress is 201.06 psi. The maximum stress lies towards the edges on shorter dimension as expected. In further subsections all variants are explained and a further analysis is made in the subsequent Chapter.



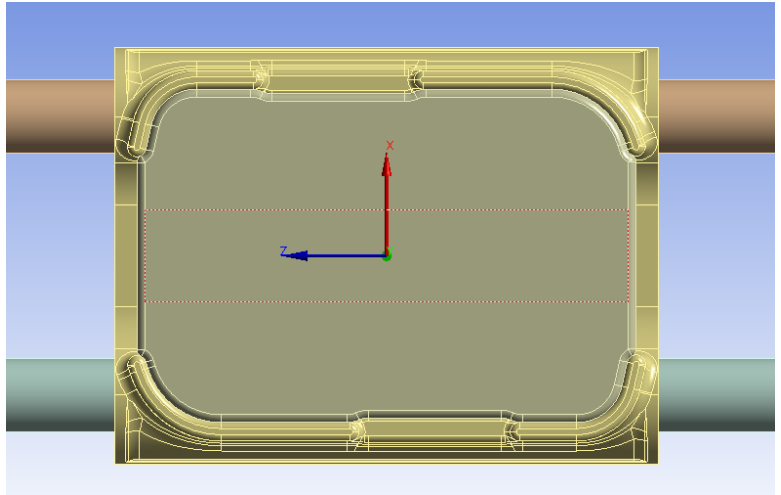


**Figure 4-6: Original Pad Ground Side**

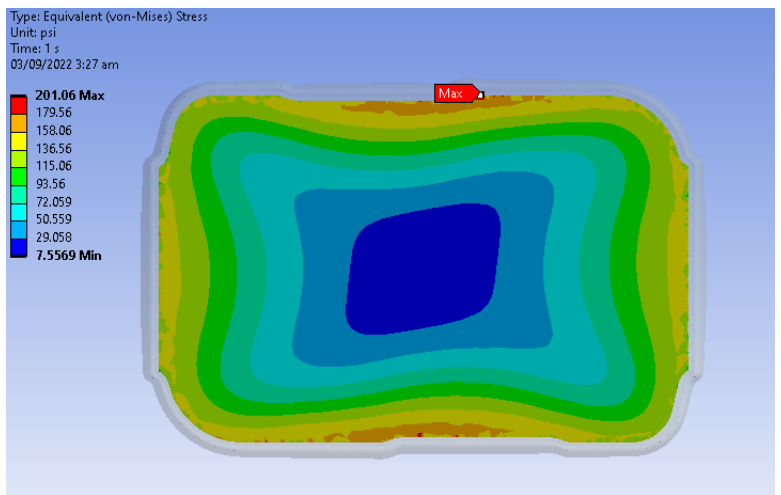


**Figure 4-7: Original Pad Ground Side Results**

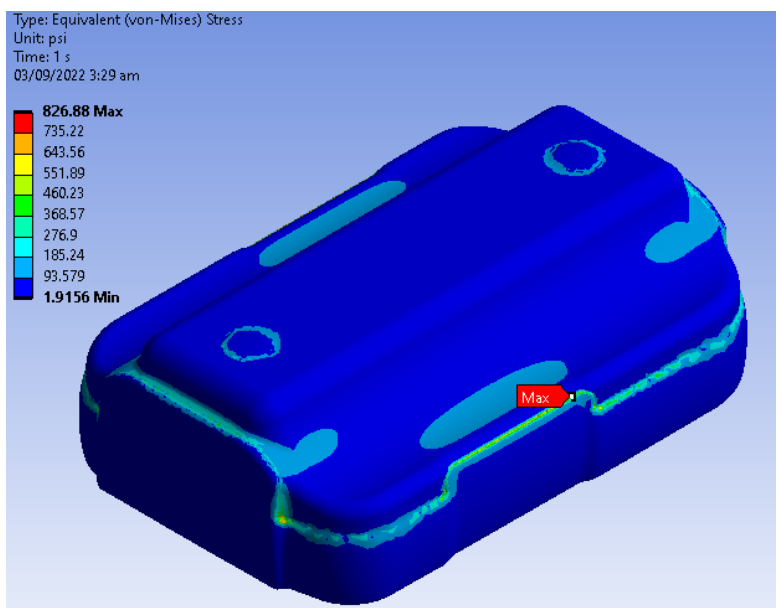


**Figure 4-8: Original Pad Results**

### 4.2.2 3-Cuts Pad Design

Three slots are cut with in the track pad from groundside for a depth of 1 inch. The volume is reduced and so the area as already explained previously in the current section. The model from groundside is shown in Figure 4-9. 3 cuts are visible in X and Z dimensions and depth is in Y dimension. Since the contact area with ground and volume is reduced therefore it is expected that the stresses induced may well be distributed in some better pattern. Load application is kept the same way as original model. The pad is made to rest on a fixed concrete floor. Ground pad is kept free to move in all DOFs. Contact settings are also kept same. Stress results at groundside and overall maximum stress on the pad are shown in Figures 4-10 and 4-11, respectively. Maximum stress on the pad is 1551.8 psi and lies on the surface that is bonded with steel body and gives a fixing impact. Maximum stress on the groundside pad lies on the internal edges in this case.

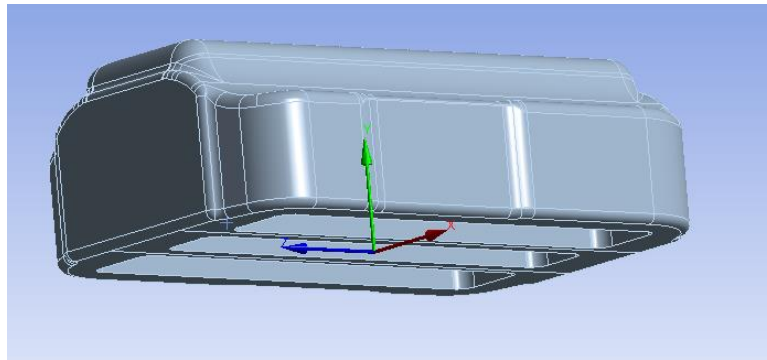


**Figure 4-9:** 3-Cuts Pad

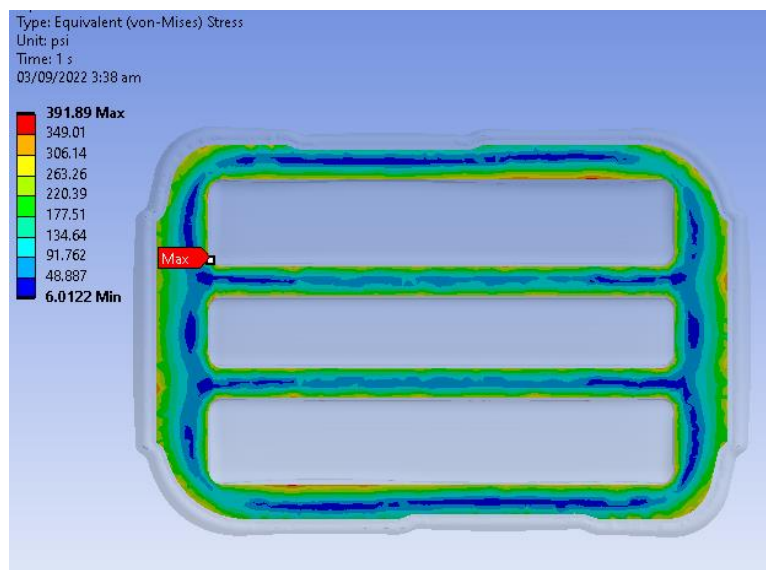


**Figure 4-10:** 3-Cuts Pad Ground Side Stress Contours

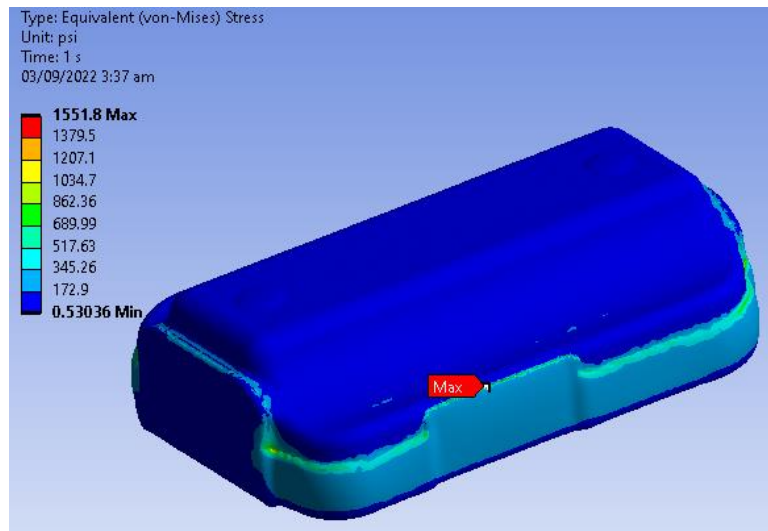


**Figure 4-11: 3-Cuts Pad Stress Contours**

### 4.2.3 4-Cuts Pad Design

Four squares are cut with in the track pad from groundside for a depth of 1 inch. The model from groundside is displayed in Figure 4-12. 4 cuts are visible in X and Z dimensions and depth is in Y dimension. The contact area and volume is further reduced to 15.903 square inch and 61.4 cubic inch. It is expected that the stresses may further increase than 3 cuts design. The stress results at groundside and overall maximum stress on the pad are shown in Figures 4-13 and 4-14, respectively. The stresses are increased as expected. Maximum stress on the pad is 1933.1 psi and lies on the surface that is bonded with steel body. Maximum stress on the groundside pad lies on the internal edges and the value is 466.4 psi.

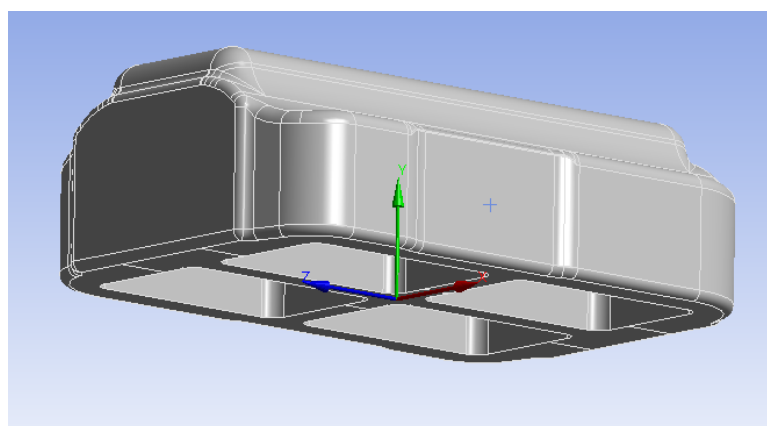


**Figure 4-12: 4-Cuts Pad**

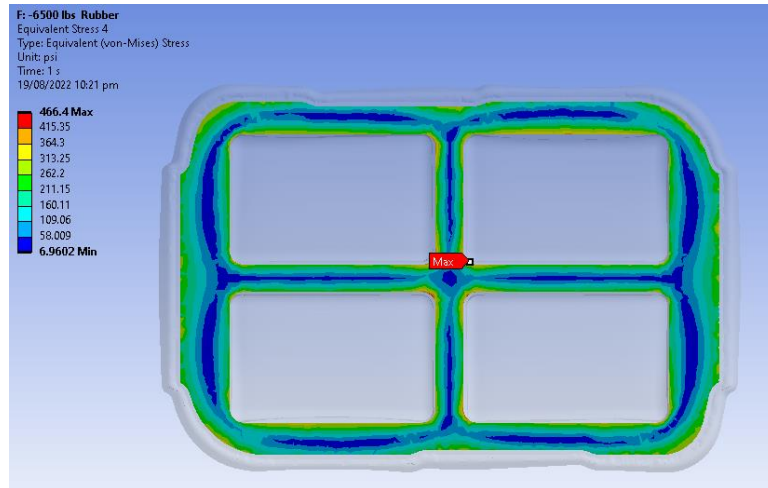


**Figure 4-13:** 4-Cuts Pad Ground Side Stress Contours

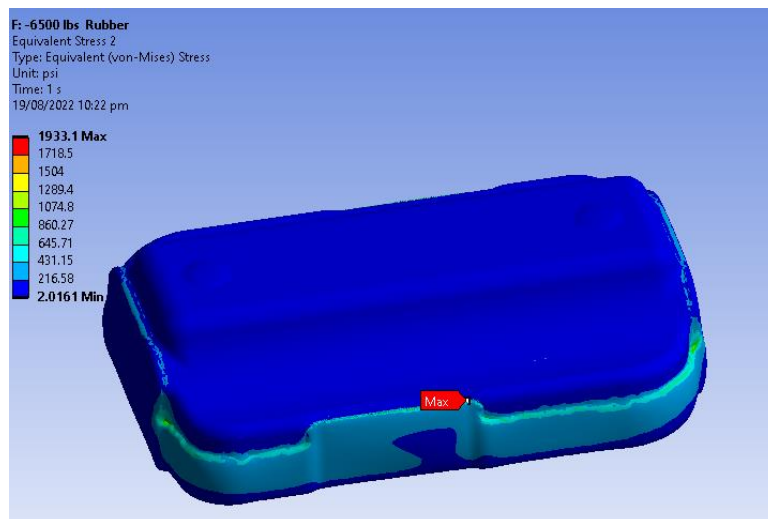


**Figure 4-14:** 4-Cuts Pad Stress Contours

#### 4.2.4 4-Lateral Cuts Pad Design

Four lateral slots are cut with in the track pad from groundside for a depth of 1 inch. The model from groundside is shown in Figure 4-15. 4 lateral cuts are visible in X and Z dimensions and depth is in Y dimension. The ground contact area is now increased to 16.863 square inch. The volume is also slightly increased to 62.6 cubic inch. Since contact area and volume is now increased so it is expected that the stresses induced will decrease. The stress results at groundside and overall maximum stress on the pad are shown in Figures 4-16 and 4-17, respectively. Maximum stress on the pad is 2073 psi and lies on the surface that is bonded with steel body. Maximum stress on the groundside pad in this case lies on the outer edges and the value is 906.98 psi. One significant observation in this case is that the stresses are further increased which is against the expected trend.

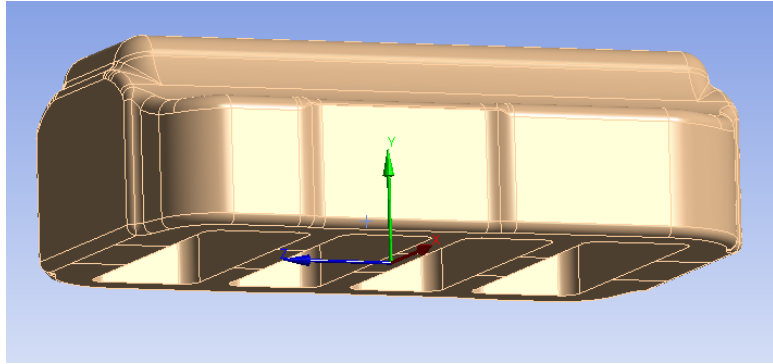


**Figure 4-15:** 4-Lateral Cuts Pad

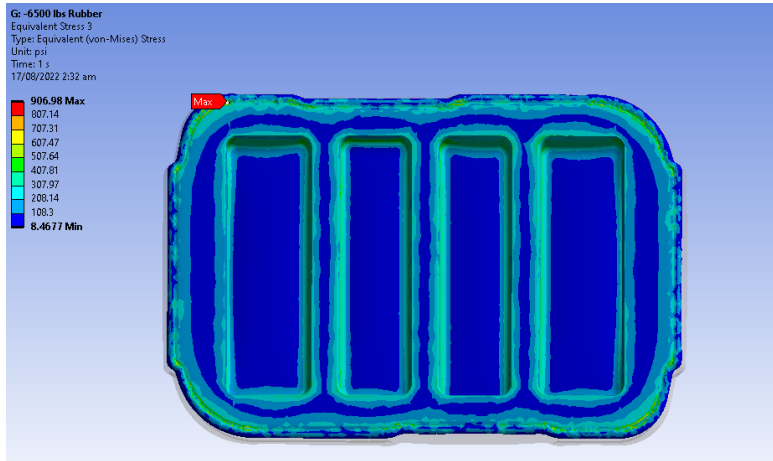


**Figure 4-16:** 4-Lateral Cuts Pad Ground Side Stress Contours

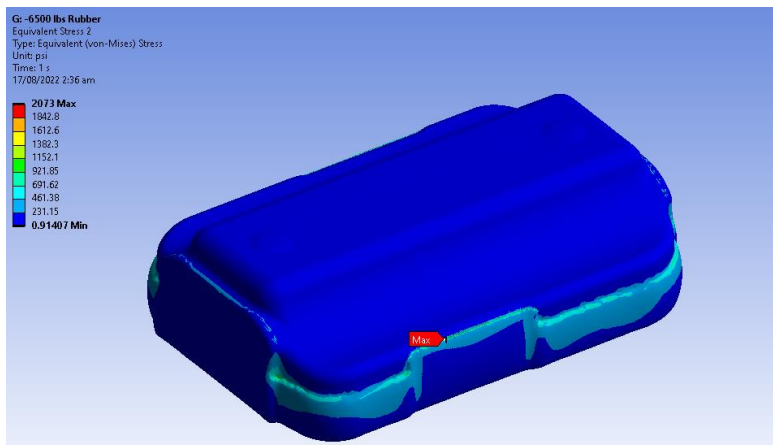


**Figure 4-17:** 4-Lateral Cuts Pad Stress Contours

#### 4.2.5 12-Cuts Pad Design

Twelve squares are cut with in the track pad from groundside for a depth of 1 inch. The model from groundside is shown in Figure 4-18. The cuts are made in a symmetric pattern from the center. The shape is visible in X and Z dimension and cut is made in Y dimension. The contact area in this case is significantly increased to 21.285 square inch. The volume is also increased to 68.06 cubic inches. The stress results at groundside and overall maximum stress on the pad are shown in Figures 4-19 and 4-20, respectively. Maximum on the stress pad is 1550.2 psi and lies on the surface that is bonded with the steel body. Maximum stress on the groundside pad lies on the outer edges and the value is 456.97 psi. The point to note is that the stresses in this case has decreased again significantly.

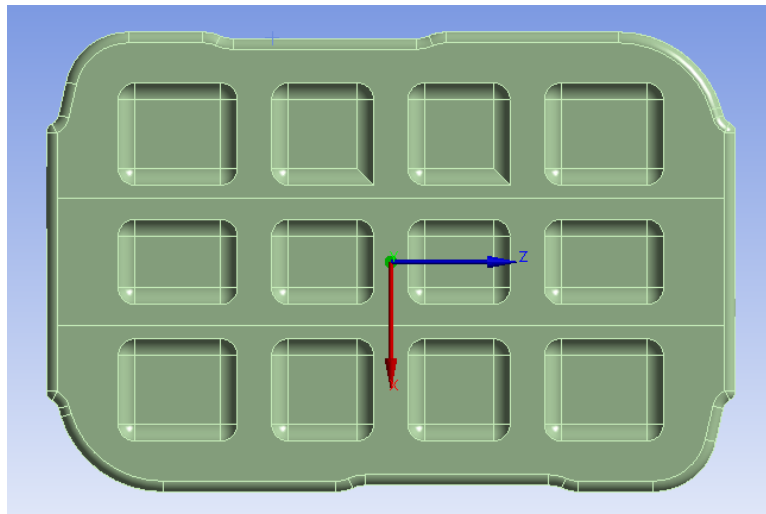


Figure 4-18: 12-Cuts Pad

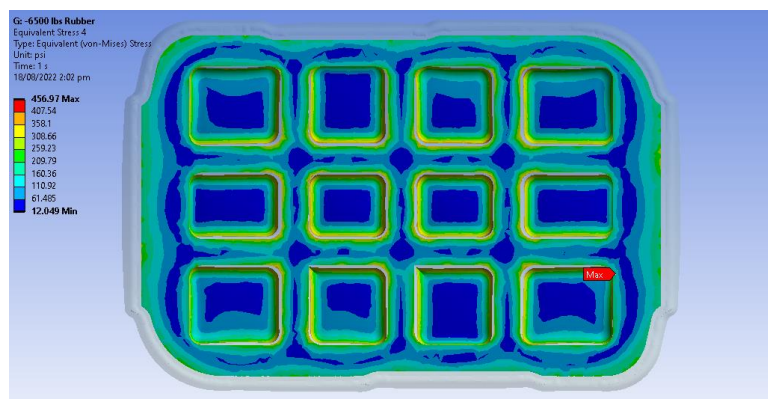
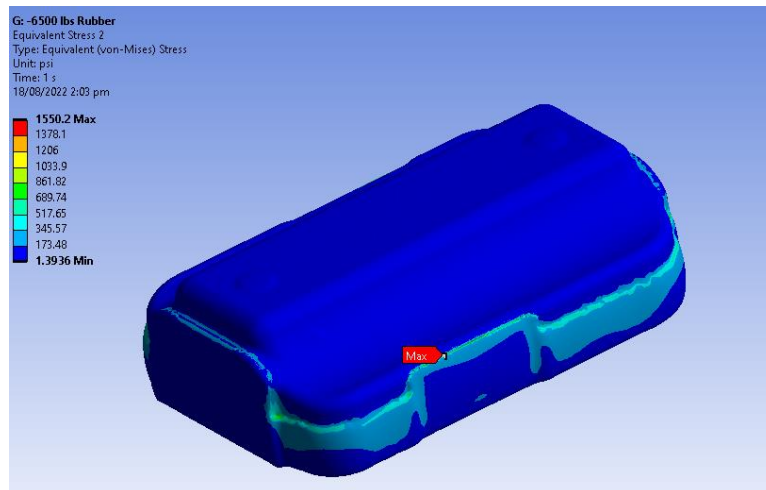


Figure 4-19: 12-Cuts Pad Ground Side Stress Contours



**Figure 4-20: 12-Cuts Pad Stress Contours**

#### **4.2.6 3-Extruded Slots Pad Design**

In the beginning of the section, it is discussed that four sub-patterns are made by removing material and one sub-pattern is made by adding material. In this variant, instead of reducing volume, the slots are extruded and volume is increased. Three slots are extruded from the ground surface for a height of 0.5 inch. The model from groundside is shown in Figure 4-21. The contact area is 21.76 square inch. The volume is increased due to material addition to 99.241 cubic inch. The stress results at groundside and overall maximum stress on the pad are shown in Figures 4-22 and 4-23, respectively. Maximum on the stress pad is 876.6 psi and lies on the surface that bonds itself with the steel body. Maximum stress on the groundside pad lies on the outer edges and the value is 715.51 psi. In this case, stress on the ground contact surface is increased however, overall stress on the pad is significantly decreased.

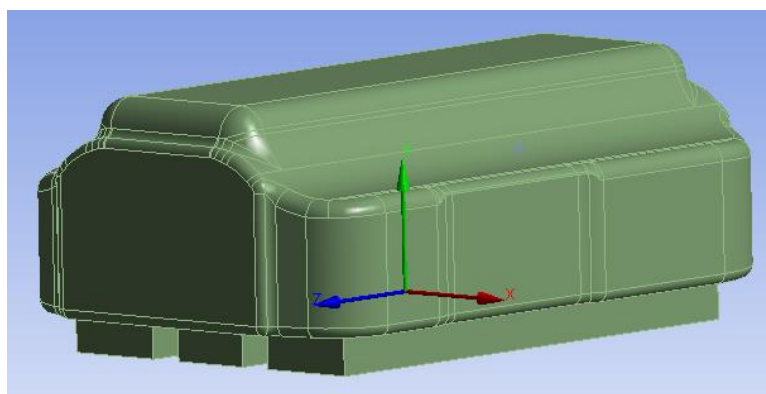


**Figure 4-21: 3-Extruded Slots Pad**

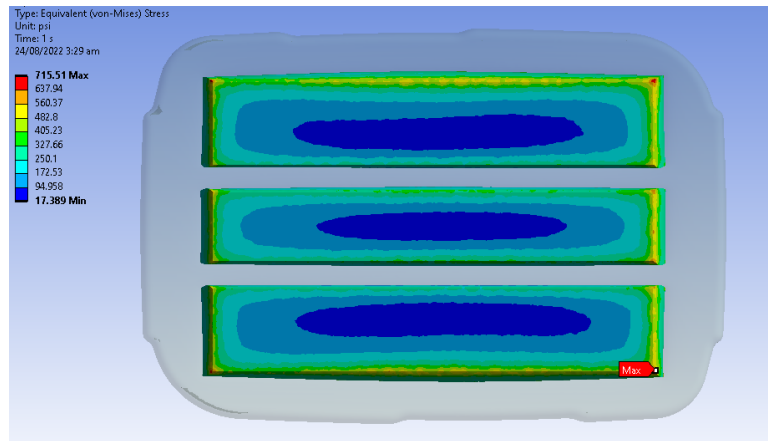


**Figure 4-22:** 3-Extruded Slots Pad Ground Side Stress Contours

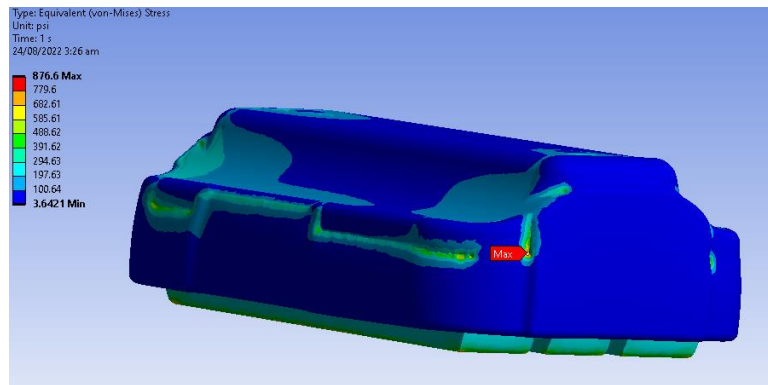


**Figure 4-23:** 3-Extruded Slots Pad Stress Contours

#### 4.2.7 Chevron Pad Design

This is the last variant and this variant is inspired from APC track pad. The design shape is changed and the volume and size of the geometry is kept almost same as per original pad to get a good comparison. The model from groundside is shown in Figure 4-24. The contact area is 35.055 square inch and the volume is 85.264 cubic inch. The stress results at groundside and overall maximum stress on the pad are shown in Figures 4-25 and 4-26 respectively. Maximum stress on the pad is 294.96 psi and lies on the surface that bonds itself with steel body. Maximum stress on the groundside pad lies on the outer edges and the value is 238.68 psi. In this case, the stresses are significantly reduced.



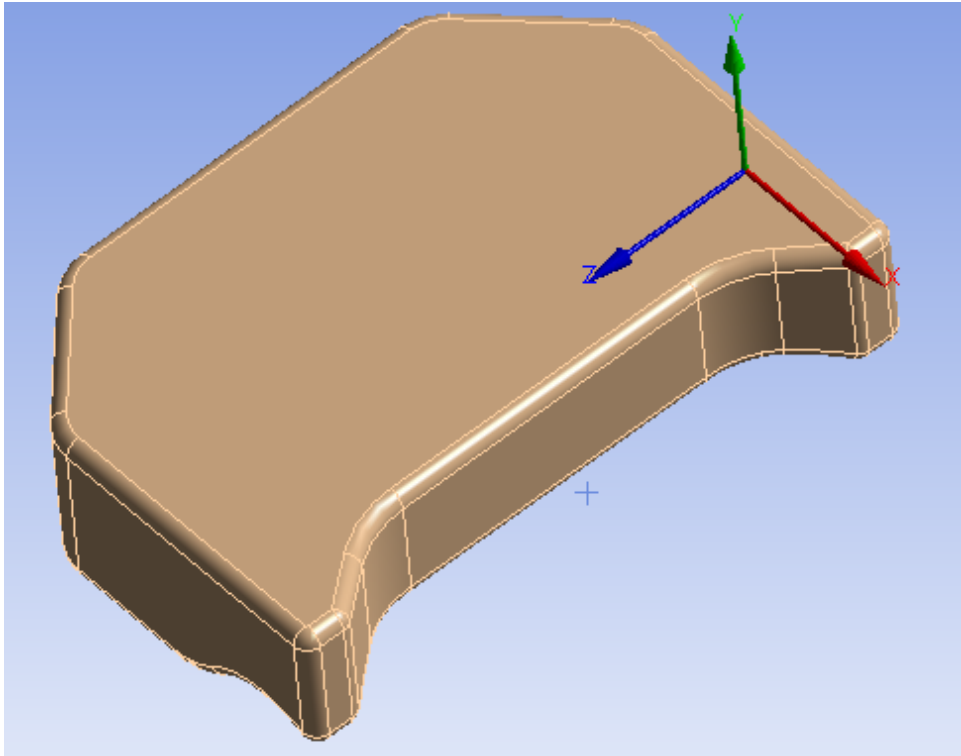


**Figure 4-24: Chevron Pad**

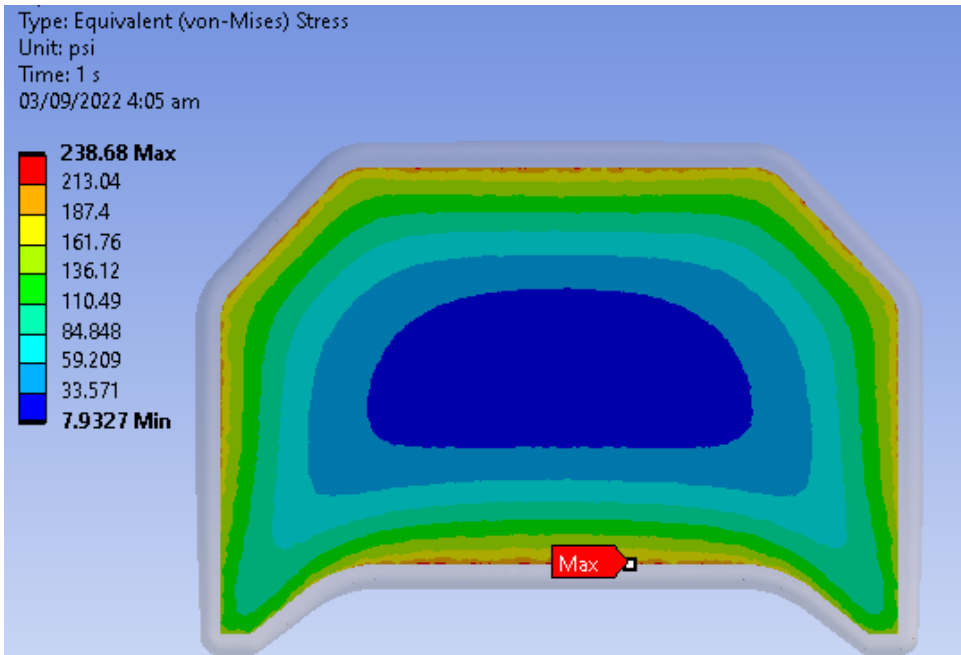


**Figure 4-25: Chevron Pad Ground Side Stress Contours**

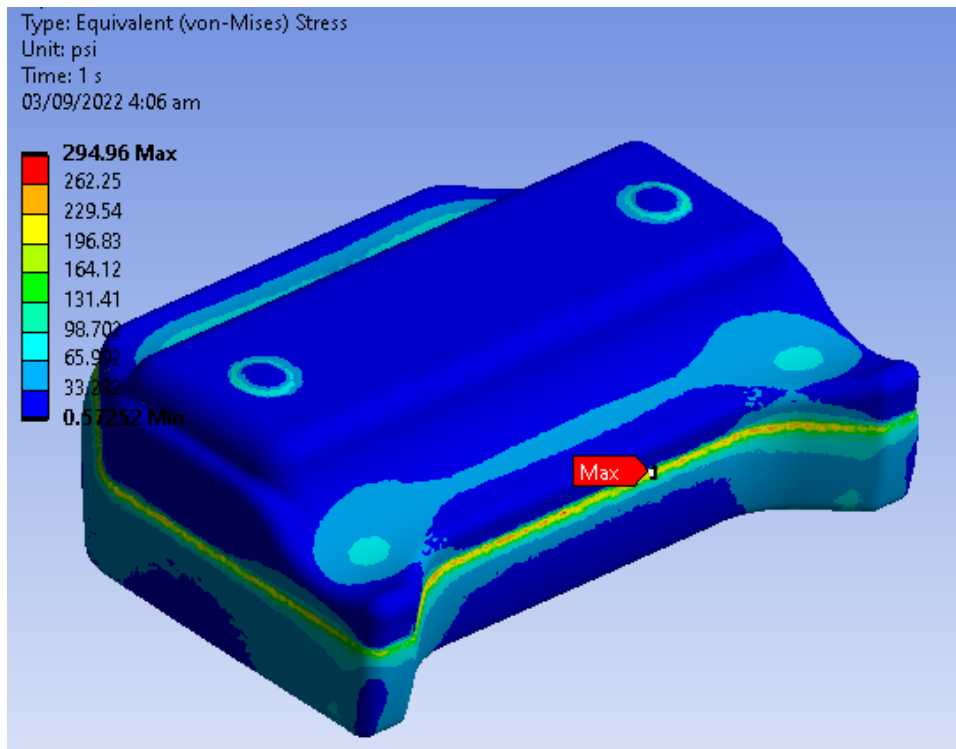


**Figure 4-26:** Chevron Pad Stress Contours

## Chapter 5

### Analysis & Discussion

#### 5.1 Material Analysis

Earlier in the chapter 4, material simulations are displayed. AISI 4140 steel performed almost similar to structural steel in the static loading model and hence it is considered just fine to use any of it for the simulations. Pin bushing material is also fixed as SBR filled with carbon black so that comparison of only pad rubber is carried out. Now answer to 1<sup>st</sup> research question is required, “What is the best suited material for ground side track pad for various loadings?”

##### 5.1.1 Material Analysis of ASTM Coupon

In hope to find some better performing locally developed rubber material, four rubber materials are selected for comparison. SBR filled with carbon black, Butyl rubber formulation, nonlinear natural rubber formulation and imported proprietary rubber formulation is compared as per ASTM standards. Comparative deformation results are displayed in Figure 4-1. The simulation is performed at various load steps starting from 20 N force. SBR and Butyl rubber formulation are linear materials and show smaller deformations, but at 40 N force these materials fail in numerical simulation. Natural rubber and proprietary rubber formulations show a near nonlinear pattern which can be seen in Figure 4-1 and the nonlinear pattern is clearly seen in Figure 4-3. At small loads corresponding to the peak strain value of less than 60%, these materials show a near linear trend and at higher loads these materials show harder behavior in comparison to lower loads as can be seen in Figure 4-3. It is also observed that natural rubber shows softer behavior than proprietary rubber and this softer behavior is magnified at higher load steps. Factor of safety of both these materials remain acceptable up to almost 150 N force as shown in Figure 4-2. Natural rubber shows better safety profile at lower load steps and the safety profile coincides with safety profile of proprietary rubber at higher load steps.

##### 5.1.2 Material Analysis of Static Loading Model

Analysis of static loading model discussed in sub section 4.1.2 is required. The model is already shown in Figure 3-2. Four rubber materials as discussed previously are used for ground pad and backer pad. Comparative deformation results are shown in Figure 4-4. Simulation is performed at four load steps starting from 6500 lbf. Figure 4-5 shows that the Butyl rubber formulation performs very low and its factor of safety remains just acceptable for only first two load steps. SBR formulation shows best factor of safety at all load steps. Natural rubber shows

matching factor of safety and proprietary rubber also shows a high enough factor of safety throughout the simulations. Natural rubber shows comparatively higher deformation and its softer behavior keeps increasing at higher loads.

### **5.1.3 Recommended Material for Pad**

SBR formulation fails at high speed operations due to cyclic loading which leads to overheating and hysteretic losses. Eventually this pad begins to crack and break apart [8]. Natural rubber is also not considered for three reasons: (a) it is highly soft and creates stability issues of the vehicle specially during steering, (b) natural rubber is less heat resistant and (c) its softer behavior is magnified at higher loads. The natural rubber formulation may be considered as a choice subject to successful experimental trials. Therefore, the original proprietary material remains the better choice amongst the simulated materials.

## **5.2 Analysis of Shape Variants**

Statistical comparison of the different proposed shapes are carried out in order to acquire the best fit shape. The task is very critical as it seeks to find a shape better than a proprietary shape. All the designed variants are generally within same definition and not much liberty is exercised in re-designing the pad due to the reasons already explained in section 5.1. In this analysis, weightage is given to stresses induced in the ground contact surface, overall stresses induced in the pad, shape, volume, weight, factor of safety and contact area.

To analyze which shape is best, a comparison of statistics are drawn from section 4.2 and shown in Table 5-1. It is expected that contact area and volume may have some significance in overall stress distribution on the track pad. Table 5-1 shows maximum stress encountered by track pad, maximum stress encountered by track pad on the ground side only, minimum factor of safety, volume, weight and overall contact area of track pad with the ground.

### **5.2.1 Shape Analysis of Static Loading Models**

It is learnt that ground contact area has no significance in terms of stress reduction. However, volume and weight has some relevance to stress reduction and therefore it does offer a choice between stress reduction and cost efficiency. Overall seven shape variants are compared including the original shape.

4-cuts and 4-lateral cuts designs are discarded due to comparatively low factor of safety. 12-cuts and 3-cuts designs has similar stress values, but 3-cut design is better because it has less stress at ground side which is primary concern in this study and it also has less weight so it is

cost effective option. 3-extruded slot design shows better overall stress value (876.6 psi) than original pad (1137.1 psi) but its stress value on ground side (715.51 psi) is much more than original pad (216.67 psi). It also has more weight and volume so it is definitely not cost efficient. Chevron pad design has much better stress values (294.96 psi) and factor of safety (8.47) than original pad. It does have a slightly higher value (238.68 psi) at ground face but it is acceptable when seen in overall context of efficiency.

**Table 5-1: Shape Comparison**

<b>Shapes Configuration</b>	<b>Max Stress (psi)</b>	<b>Max Stress on the Groundside Face (psi)</b>	<b>Factor of Safety</b>	<b>Volume (in<sup>3</sup>)</b>	<b>Weight (lbs)</b>	<b>Ground Contact Area (in<sup>2</sup>)</b>
4-Cuts	1933.1	466.4	1.29	61.4	2.62	15.903
4-Lateral Cuts	2073	906.98	1.2	62.6	2.67	16.863
12-Cuts	1550.2	456.97	1.61	68.06	2.90	21.285
3-Cuts	1551.8	391.8	1.61	62.7	2.68	16.908
3-Extruded Slots	876.6	715.51	2.85	99.241	4.24	21.76
Original Pad	1137.1	216.67	2.2	88.3	3.77	38.563
Chevron Pad	294.96	238.68	8.47	85.264	3.64	35.055

### 5.2.2 Stress in Steel Track Body

There is one more aspect to be studied before finalizing the choice of shape. Overall what happens to steel track body carrying this track pad. Does it also behave better or otherwise? A comparison is therefore necessary. In case of original pad design, maximum stress on steel body lies at the edge of the bolt hole (30695 psi) as shown in Figure 5-1. The factor of safety of this body is very less (1.1813) at static load of 6500 lbf which is alarming. On the other hand, stress in steel track body of chevron track is 8487.8 psi (Figure 5-2) with factor of safety is 4.2719.

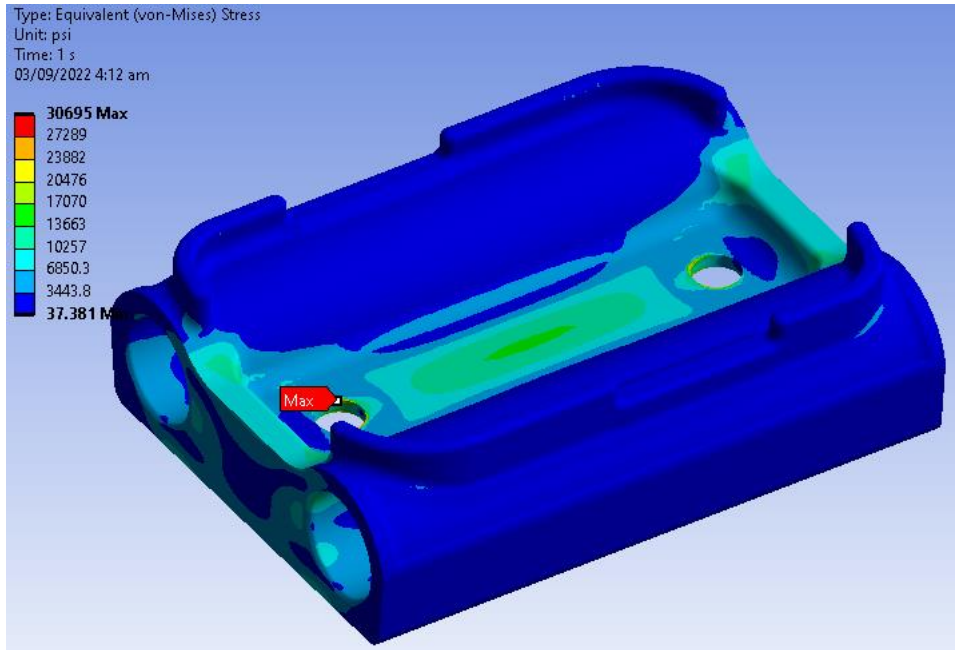


**Figure 5-1:** Original Pad Design Steel Body

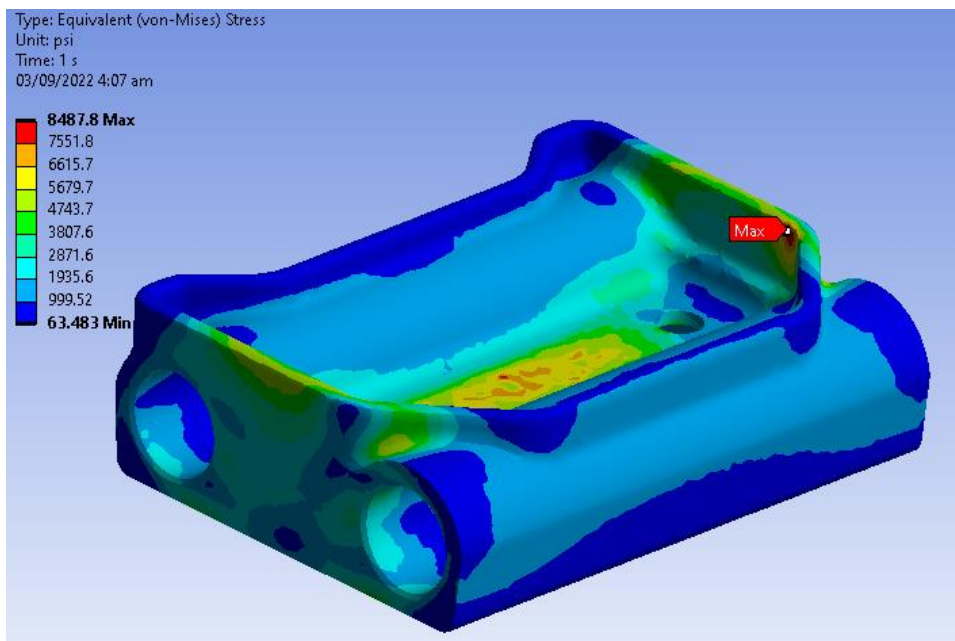


**Figure 5-2:** Chevron Pad Design Steel Body

### 5.2.3 Chevron Pad vs Original Pad Comparison

Stress in chevron pad is significantly reduced. The question arises why is such a significant decrease as general dimensioning is kept almost same. We look into details of stress contours of original pad ground side as shown in Figure 5-3 and stress contours on groundside of chevron

pad in Figure 5-4. The maximum stress lies towards the shorter dimension. If we closely see the stress contours in original pad, we find that the stress distribution is concentrated towards maximum stress point as shown in red, orange and yellow contours. These stresses are of the order of 146.94 psi to 216.67 psi. The majority of the stresses on the surface are in the range of 30.709 to 146.94 psi as shown by various contour bands. On the other hand if we closely see the surface of chevron pad, we observe that the stresses are not concentrated at some particular point, instead stresses are evenly distributed everywhere. The peak stresses are taken by almost all the edges as can be seen in red, orange, yellow and light green contours. These stresses are of the order of 136.12 psi to 238.68 psi. The majority of the surface bears lighter stresses which are more uniformly distributed than original pad. These stresses are of the order of 7.9327 psi to 136.12 psi which is obviously better than original pad. The same is validated by iso lines on the chevron pad as shown in Figure 5-5. The most of the area is undergoing stresses less than 136 psi line.

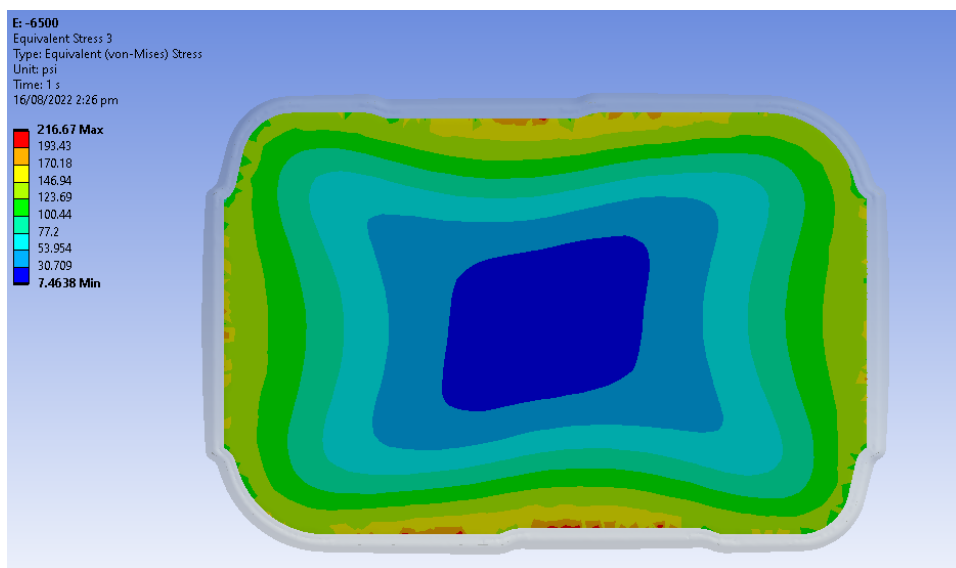


**Figure 5-3:** Original Pad Groundside Stress Contours

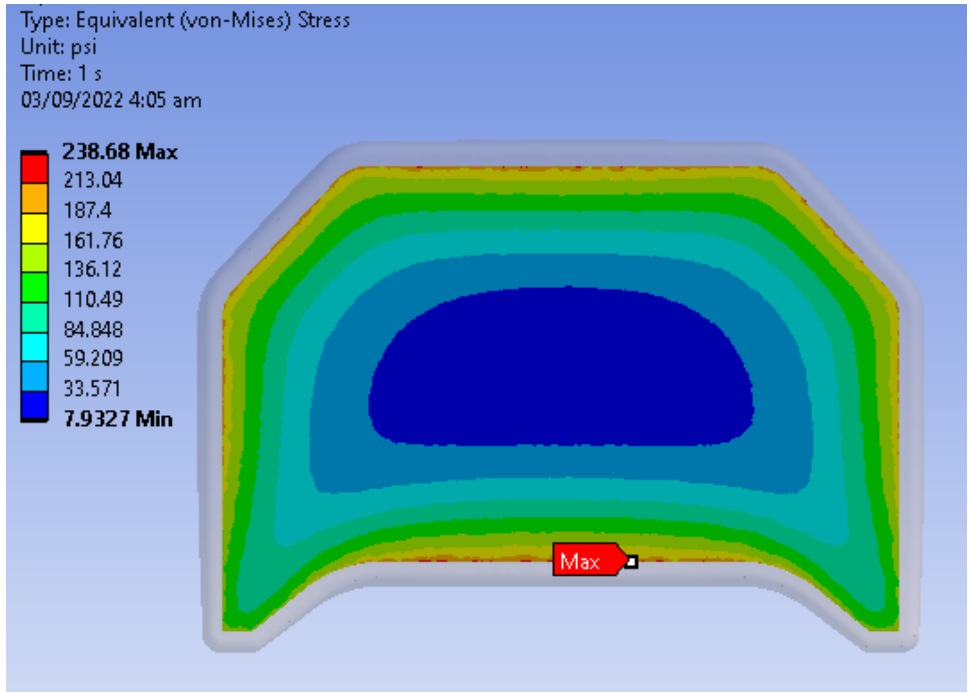


**Figure 5-4: Chevron Pad Groundside Stress Contours**

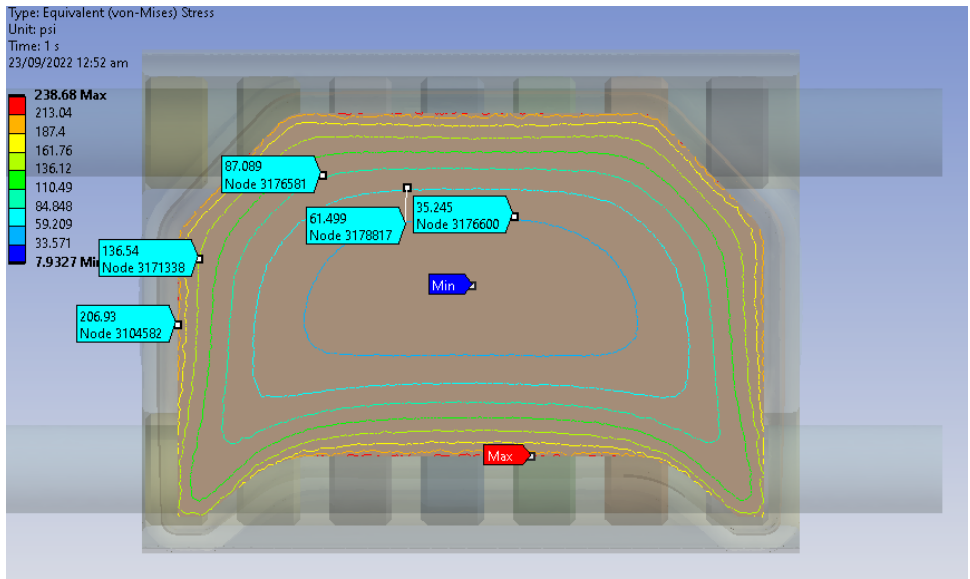


**Figure 5-5: Chevron Pad Groundside Stress Iso Lines**



We now compare the stress distribution in chevron and original pad steel bodies. Figure 5-6 shows stress contours in steel body of original pad. Blue contour is taking most of the space on this body (almost 60 percent), the stresses are of the order of 22.569 psi to 3356.2 psi. The middle stress bands is covering the central strip. The stresses in these bands are of the order of 3356.2 psi to 20024 psi. The peak stresses are at the edges of the bolt hole and is of the order of 20024 psi to 30025 psi. We now look at the stress distribution in Chevron pad steel body in Figure 5-7. The majority of the stresses are evenly distributed, these stresses are shown by multiple light blue contours throughout the body. The stresses in these contours are of the order of 999.52 psi to 3807.6 psi. The peak stress is occurring at the corner skirting and a red spot in the center also showing stress on the higher side. A small central area is covered by red, orange, yellow and green contours and represents the stresses in the order of 3807.6 psi to 8487.8 psi. Seeing the overall distribution we can conclude that the stress distribution is better in chevron style and stress distribution is high and concentrated in original design.

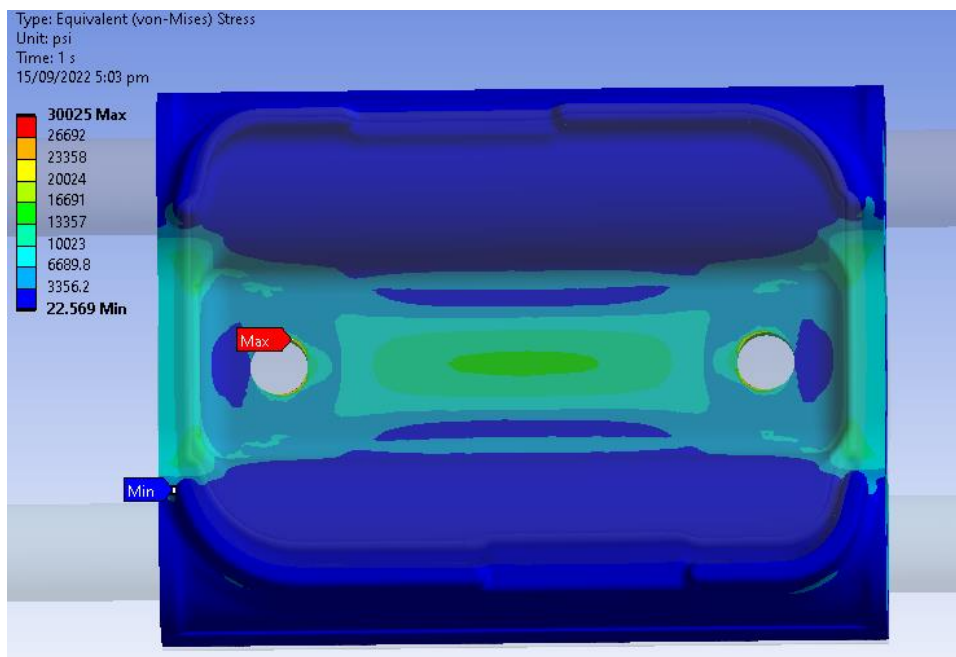


**Figure 5-6:** Original Design Steel Body Stress Contours

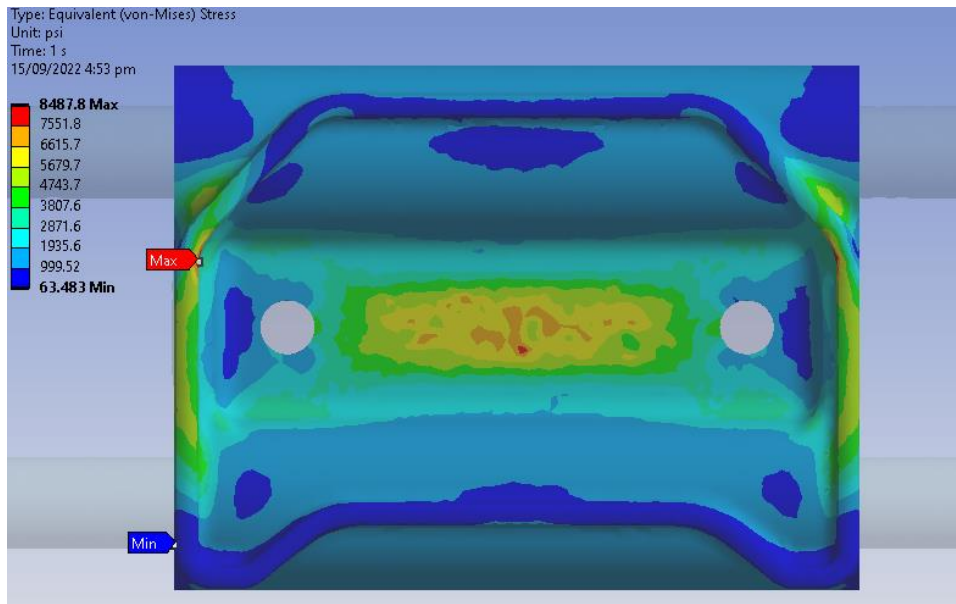


**Figure 5-7:** Chevron Design Steel Body Stress Contours

#### 5.2.4 Recommended Shape

Chevron Pad configuration is having best factor of safety with better weight and volume, therefore it is a recommended choice.

### 5.3 Dynamic Loading Analysis

Chevron pad design recommended in previous sections is required to undergo a dynamic loading analysis to further validate the recommended design. Dynamic CAD model is explained in section 3.1.1 and shown in Figure 3-1. A three pair pad-track link is derived from tank track for FEM analysis. Dominant role of track loading is compression, but in actual track also undergoes shear due to tension in the track. To simulate the track tension, the model is modified a little. The tensile force of 3250 lbf is applied at both ends of the model as shown in Figure 5-8.

It is assumed that the tank is moving at a constant velocity of 60 kmph (16.66666 m/s). The road wheel rolling over the backer track pad is to be simulated. The radius of the road wheel is 14.5 inches which gives angular velocity of 45.2 radians per second or 7.2 revolutions per second. The time step is calculated from velocity of tank. The model has to travel a distance of 18 inches with a velocity of 60 kmph, which gives total time of 0.03 seconds. The loading of 6500 lbs is traversed on the backer track pad of the model at this time step of 0.03 seconds for velocity of 60 kmph. The traversing forces are shown on the backer pads in Figure 5-8. The track is set on the concrete floor which is fixed.

FEA results are obtained which represents the occurrence of maximum stress at steel track body at the time  $t=0.009$  seconds as shown in Figure 5-9. Figure 5-10 shows the stresses produced in central ground pad. Since model contains 3 pair of pad track links so it is appropriate to consider the central track pad for analysis. The maximum stress on the central ground side track pad occurs at time  $t=0.0105$  seconds and value is 44.533 psi which is very well within the safe region. The overall safety factor of the track bodies is 8.76 which is highly stable. It is worth mentioning here that the maximum stress in the pad is not produced at the time of peak load on that pad. The peak load on the pad occurs at 0.015 seconds and the maximum stress occurs before that. This disparity is probably due to the shearing force present or due to the asymmetric design of the pad in track traversing dimension.

Chevron pad design shows its strength during this dynamic analysis and therefore it is a good choice for use.

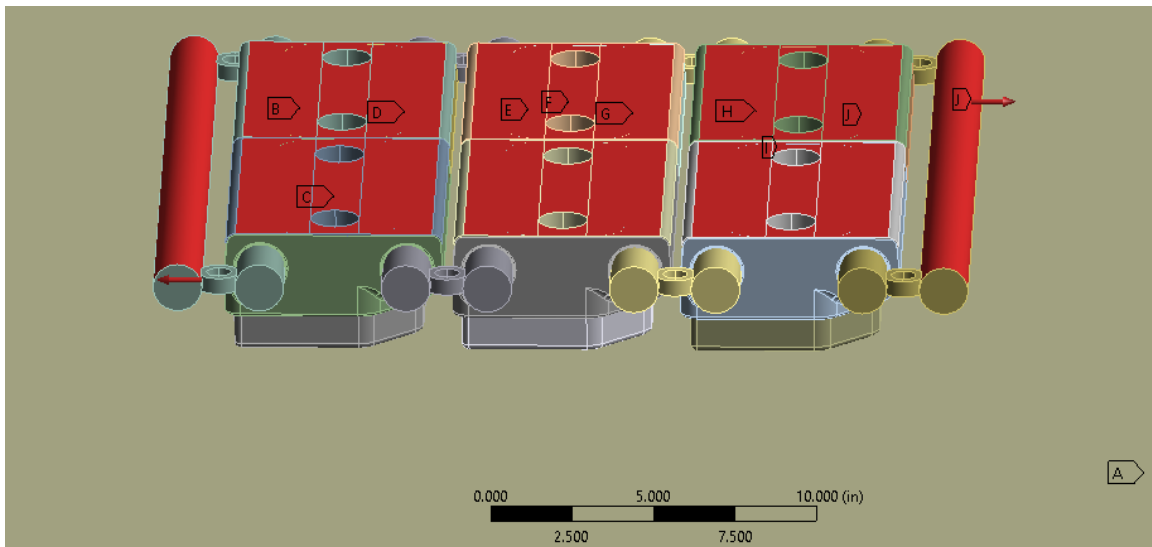


**Figure 5-8:** Dynamic Loading Model with Applied Forces

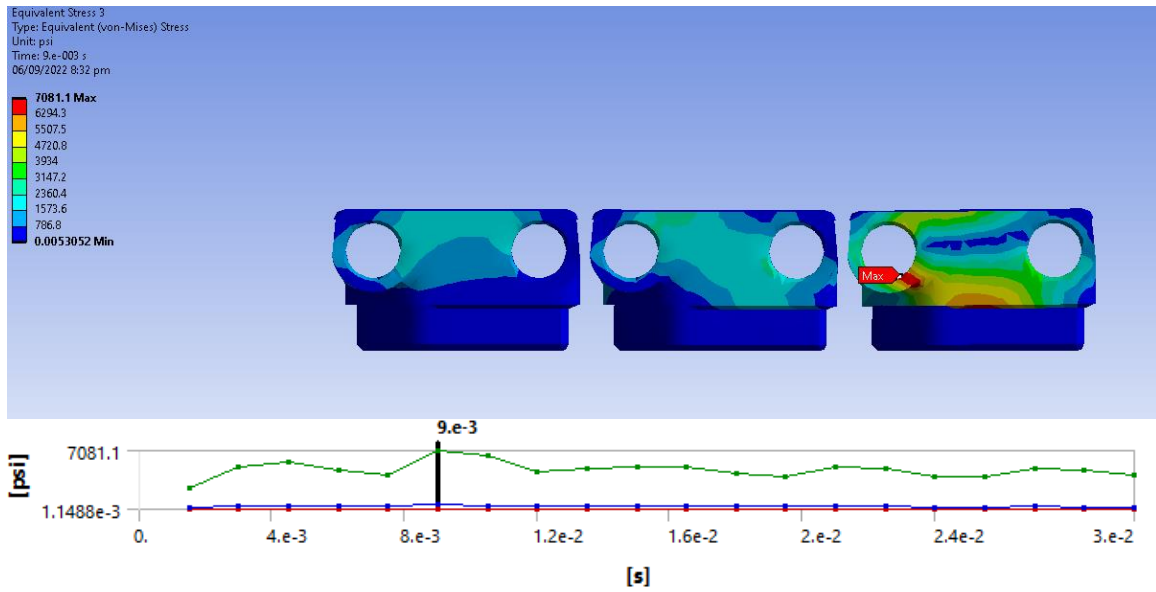


**Figure 5-9: Maximum Stress in Dynamic Model**

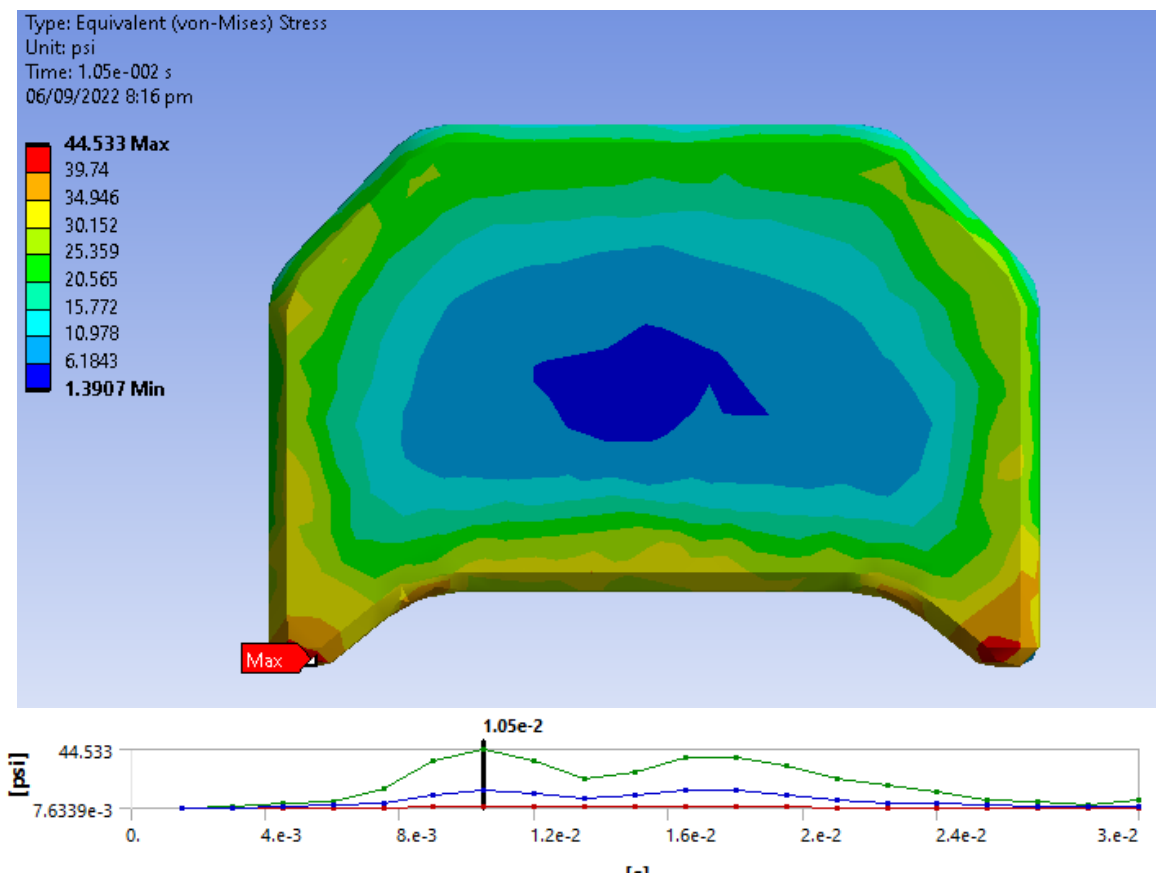


**Figure 5-10: Maximum Stress in Central Track Pad**

## Chapter 6

### Conclusion & Future Work

#### 6.1 Conclusion

This research focused the track pad analysis as its significance is already defined in chapter 1. Overall material analysis and shape analysis is conducted with a view to find a better performing combination of material and shape. Shape optimization is not discussed in this study, however, a total of four materials and seven shapes are compared to achieve a better track pad design.

In chapter 3, FEA results are displayed which suggested that more materials should have been opted for this study to reach a better material choice. Material testing was not the primary scope of this work and unfortunately, data related to material testing could not be made available for FEA. Material analysis of the four materials discussed in this study has led to the conclusion that the original proprietary material has remained the best choice, amongst the analyzed materials.

It was expected right from the conception of this study that material and shape variation may reduce the stresses induced in the track and track pad. Seven shapes are analyzed in the study for this purpose. Initially minor changes are carried out in the original track pad design. Volume is reduced from the track pad to see the impact on stresses and it is observed that reduction in volume increases the stresses in the pad and reduces the factor of safety. In another attempt, volume is added by extruding the track pad and stresses induced becomes better and factor of safety is enhanced.

In a different design inspired by other tracked vehicles, chevron track pad is designed. While designing this pad, general dimensioning is kept almost same as original pad to get a true comparison. This track pad performs better and stresses are lesser than the original pad. The same design is simulated with dynamic forces at constant velocity of 16.67 meter per second. This dynamic analysis also validated the design choice and hence this design becomes the recommended choice.

In this study, the concept is positively proved that a better design feasibility of this existing track pad exist. Chevron pad design is definitely better but it is not an optimized design. An optimized solution to the problem may be obtained with further efforts.

## **6.2 Future Work**

There are some recommendations made for the future work due to lack of computational power or unavailability of enough time to conduct additional study beyond what has already been done.

Lack of material data has remained a major concern during the thesis. Material testing may be carried out for available materials in detail. A cyclic loading analysis may be carried out for life cycle analysis of candidate material. Further, a non-linear analysis may be carried out for non-linear materials. Dynamic loading analysis is considered for constant speed case, the same may be conducted for cases of vehicle accelerating and decelerating, the values of deceleration data identified by Keays may be used [9]. Dynamic loading analysis may be carried out for track vehicle crossing different types of obstacles. Dynamic loading analysis may be carried out for track vehicle making a steer at high speeds. A FEM model for complete track may be developed for vibrational analysis and explicit dynamic analysis.

## References

- [1] M. R. Gurvich, "On challenges in structural analysis of rubber components: Frictional contact," *Journal of Elastomers and Plastics*, vol. 39, no. 1, pp. 53–67, Jan. 2007, doi: 10.1177/00952443070067387.
- [2] US Army Tank Automotive Command, "Development of fiber reinforced tracked pad materials," Michigan, 1986.
- [3] C. G. Pergantis, "Thermographic field-inspection study on M1 main battle tank track systems," *Thermosense XIV: An Intl Conf on Thermal Sensing and Imaging Diagnostic Applications*, vol. 1682, no. April 1992, pp. 239–247, 1992, doi: 10.1117/12.58541.
- [4] J. Wang, \* -Dagang Sun, -Shizhong Liu, -Yong Song, -Bijuan Yan, and -Bao Sun, "Prediction of heat accumulation of symmetrical rubber buffer on track-type bulldozer," *Engineering Review*, vol 37, no. 3, pp. 281-288, 2017.
- [5] Z. T. Satterfield, "Design of a meta-material with targeted nonlinear deformation response," Clemson University, 2015.
- [6] N. M. Kulkarni, "Design optimization of tank track pad meta-material using the cell synthesis method," Clemson University, 2016. Available: [https://tigerprints.clemson.edu/all\\_theses/2414](https://tigerprints.clemson.edu/all_theses/2414)
- [7] Z. Satterfield, N. Kulkarni, G. Fadel, G. Li, N. Coutris, and M. P. Castanier, "Unit cell synthesis for design of materials with targeted nonlinear deformation response," *Journal of Mechanical Design, Transactions of the ASME*, vol. 139, no. 12, Dec. 2017, doi: 10.1115/1.4037894.
- [8] S. J. Franklin, "Design of meta-material tank track system with experimental testing and sensitivity analysis of additively manufactured meta-material backer pads," Clemson University, 2018.
- [9] Keays, R.H., "Analysis of armoured vehicle track loads and stresses, with considerations on alternative track materials," Materials research labs Ascot Vale (Australia), 1989.
- [10] Medalia, A.I., Alesi, A.L. and Mead, J.L., "Pattern abrasion and other mechanisms of wear of tank track pads," *Rubber chemistry and technology*, 65(1), pp.154-175, 1992.
- [11] US Army Tank Automotive Command, "Development and Fabrication of Track Pads," Michigan, 1986.

- [12] D. Ostberg and B. Bradford, “Ground vehicle systems engineering and technology symposium (GVSETS) impact of loading distribution of Abrams suspension on track performance and durability,” 2009.
- [13] M. Campanelli, A. A. Shabana, and J. H. Choi, “Chain vibration and dynamic stress in three-dimensional multibody tracked vehicles,” *Multibody Syst Dyn*, vol. 2, no. 3, pp. 277–316, 1998, doi: 10.1023/A:1009758701296.
- [14] “Abaqus Analysis User’s Manual Version 6.14.”
- [15] R. M. Walser, “Electromagnetic metamaterials,” *Proc. SPIE* vol. 4467, 2001. Available: <http://spiedl.org/terms>
- [16] V. S. Dangeti, “Identifying target properties for the design of meta-material tank track pads,” Clemson University, 2014.
- [17] S. Tang, S. Yuan, J. Hu, X. Li, J. Zhou, and J. Guo, “Modeling of steady-state performance of skid-steering for high-speed tracked vehicles,” *J Terramech*, vol. 73, pp. 25–35, 2017, doi: 10.1016/j.jterra.2017.06.003.
- [18] J. Y. Wong and C. F. Chiang, “A general theory for skid steering of tracked vehicles on firm ground,” *Proceedings of the Institution of Mechanical Engineers, Part D: Journal of Automobile Engineering*, vol. 215, no. 3, pp. 343–355, 2001, doi: 10.1243/0954407011525683.
- [19] Q. Rui, H. Y. Wang, Q. L. Wang, J. Guo, T. G. Zou, and L. Wan, “Analysis and experiment of tracked vehicle steering torque based on shear stress model,” *Binggong Xuebao/Acta Armamentarii*, vol. 36, no. 6, pp. 968–977, Jun. 2015, doi: 10.3969/j.issn.1000-1093.2015.06.002.
- [20] H. S. Ryu, D. S. Bae, J. H. Choi, and A. A. Shabana, “A compliant track link model for high-speed , high-mobility tracked vehicles,” no. October 1999, pp. 1481–1502, 2000.
- [21] K. Lee, “A numerical method for dynamic analysis of tracked vehicles of high mobility,” *KSME International Journal*, vol. 14, no. 10, pp. 1028–1040, 2000, doi: 10.1007/BF03185057.
- [22] T. Nabaglo, J. Kowal, and A. Jurkiewicz, “Construction of a parametrized tracked vehicle model and its simulation in MSC.ADAMS program,” *Journal of Low Frequency Noise Vibration and Active Control*, vol. 32, no. 1–2, pp. 167–174, 2013, doi: 10.1260/0263-0923.32.1-2.167.



- [23] T. Nabag, A. Jurkiewicz, and J. Kowal, “Modeling verification of an advanced torsional spring for tracked vehicle suspension in 2S1 vehicle model,” vol. 229, 2021, doi: 10.1016/j.engstruct.2020.111623.
- [24] S. Banerjee, V. Balamurugan, M. Sunil, and G. Srinivasan, “Transient dynamic finite element analysis of the air-defence weapon system mount assembly of tracked vehicle,” *Procedia Eng*, vol. 144, pp. 382–389, 2016, doi: 10.1016/j.proeng.2016.05.147.
- [25] Static Structural, Software Package, Ver, 2022 R1, ANSYS, Inc, Lebanon, NH, 2022.